Aus der Klinik für Nephrologie
der Medizinischen Fakultät Charité – Universitätsmedizin Berlin

DISSERTATION

Identification of protein biomarkers for chronic kidney disease progression using state-of-the-art proteomics approaches

zur Erlangung des akademischen Grades
Doctor rerum medicinalium (Dr. rer. medic.)

vorgelegt der Medizinischen Fakultät
Charité – Universitätsmedizin Berlin

von

Szymon Filip

aus Lębork, Poland

Datum der Promotion: 09/12/2016

Table of contents

1. Abstract

Proteins are essential for performing the vital functions in the organism and changes in the homeostasis reflect the disease state. Large-scale proteomics studies are commonly performed for the identification of protein biomarkers of complex diseases as chronic kidney disease (CKD), which is the gradual decrease in renal function and is recognized as a major public health burden. Novel biomarkers that allow improved detection at early stages and prognosis of disease development are still needed. Therefore, this thesis is aiming at the identification of proteomics changes related to CKD progression.

The first part of the thesis focuses on the identification of proteomics changes of the plasma of patients suffering from CKD. We analysed the plasma proteome of patients with CKD stage 2–4 as well as CKD stage 5 with or without haemodialysis, using liquid chromatography coupled to mass-spectrometry (LC–MS/MS) and enzyme-linked immunosorbent assay (ELISA). Pathway analysis confirmed the modification of known processes involved in CKD pathophysiology, including deregulation of fibrin-clot formation and complement activation. Moreover, levels of complement factor D, lysozyme C and leucine-rich alpha-2 glycoprotein were identified to increase with CKD progression.

The second part of the thesis focuses on the optimization of the protocol for the identification of CKD progression biomarkers in urine. We compared the reproducibility and efficiency in depleting high-abundance proteins of different methods, using urine samples from CKD patients and controls. Decrease in the amount of albumin and other targets following sample treatment was observed. However, the number of protein identifications did not increase after using these methods.

The third part concentrates on the identification of CKD biomarkers in tissue samples using matrix-assisted laser desorption/ionization mass-spectrometry imaging (MALDI-MSI). Fresh frozen renal tissue from patients and controls were analysed to detect molecular signatures of primary glomerulonephritis. MALDI-MSI can generate molecular signatures capable to distinguish between normal kidney and idiopathic glomerulonephritis, with specific signals representing potential indicators of CKD development. A peak with m/z=4048 was identified as an α-1-antitrypsin (A1AT) peptide and the protein was shown to be localized to the podocytes within sclerotic glomeruli by immunohistochemistry. Additionally, correlation of MALDI-MSI findings with urinary proteomics identified identical A1AT peptide as up-regulated in CKD patients prone to fast progression to further stages of the disease.

Each of these studies offers novel insights relative to CKD progression. These results will collectively allow for elucidation of the disease progression mechanism, contributing to the discovery of novel therapeutic targets.

Zusammenfassung

Proteine sind verantwortlich für die wichtigsten Funktionen im Organismus, der Homöostase und des Krankheitszustandes. Großangelegte Proteomstudien sind unter anderem mit dem Ziel durchgeführt worden, neue Protein-Biomarkern komplexer Erkrankungen wie beispielsweise der chronischen Nierenerkrankungen (CKD) zu identifizieren. Gegenwärtige werden Biomarker zur Frühdiagnostik und Progression der CKD intensiv gesucht Das Ziel der vorliegenden Dissertation ist es daher einen Beitrag zur Identifizierung von proteomischen Änderungen im Rahmen der CKD zu leisten und dadurch neue Biomarker zu beschreiben zu könen.

Der erste Teil der Dissertation konzentriert sich auf die Identifizierung von proteomischen Veränderungen im Plasma von CKD-Patienten. Es wurde das Plasma-Proteom von CKD-Patienten in CKD Stadium 2-4 und 5 mit oder ohne Hämodialyse mittels Flüssigkeitschromatographie mit Tandem-Massenspektrometrie (LC-MS/MS) und enzymgekoppelter Immunadsorptionstest (ELISA) untersucht. Pathway-Analysen bestätigten Modifikation der bekannten Stoffwechselprozesse, die in der CKD-Pathophysiologie beteiligt sind. Dazu gehört die Deregulierung der Fibrin-Gerinnselbildung und die Aktivierung des Komplements. Außerdem konnte festgestellt werden, dass das Niveau von Komplementfaktor D, Lysozym C und leucin-reichen alpha-2-Glykoprotein mit der CKD-Progression erhöht wird.

Der zweite Teil der Dissertation konzentriert sich auf die Optimierung des Protokolls zur Identifizierung von CKD-Progressionsbiomarkern im Urin. In dieser Studie verglichen wir die Reproduzierbarkeit und Effizienz der Abreicherung von hochkonzentierten Proteine mit verschiedenen Methoden unter Verwendung der Urinproben von CKD-Patienten und Kontrollen. Abnahme der Menge von Albumin und anderen Analyten nachfolgend der Probenbehandlung wurde beobachtet. Allerdings bliebt die Anzahl der Protein-Identifikationen konstant.

Der dritte Teil der vorliegenden Arbeit fokussiert sich auf die Identifizierung von CKD-Biomarkern in Gewebeproben unter Verwendung der Technik des „Matrix-unterstützter Laser-Desorption/Ionisation-Bildgebung“ (MALDI-MSI). Frisches gefrorenes Nierengewebe von Patienten und Kontrollen wurden analysiert um molekulare Signaturen von primären Glomerulonephritis zu erkennen. Mittels MALDI-MSI konnten molekulare Signaturen generiert

werden, die zwischen der normalen Niere und idiopathische Glomerulonephritis unterschieden, mit Massensignalen, die potenzielle Indikatoren für die CKD-Entwicklung darstellen. Ein Massensignal bei 4048 (m/z) wurde als ein α-1-Antitrypsin (A1AT) Peptid identifiziert und es wurde durch Immunhistochemie gezeigt, dass das Protein in den Podozyten innerhalb sklerotischer Glomerulie lokalisiert ist. Zusätzlich führte die Korrelation von MALDI-MSI Ergebnissen mit Urin- Proteomik zur Identifizierung eines A1AT-Peptids, das bei CKD-Patienten hochreguliert war.

Jede dieser Studien bringt neue Erkenntnisse in Bezug auf die CKD-Progression. Diese Ergebnisse werden die Aufklärung der Progressionsmechanismus der Krankheit erlauben und einen Beitrag zur Entdeckung neuer therapeutischer Ziele leisten.

2. Introduction

Proteins are essential for biological process, since they represent the expression of genetic information and the effect of environmental factors. They are involved in dynamic processes such as metabolism, but they can also fulfil static structural roles. Large-scale analyses of proteins using state-of-the-art technologies is thought to enable a deeper understanding of not only physiological, but also pathological processes [1]. Since the number of unique proteins present in the human body is vast, while pathological changes may only be associated with a fraction of them, attempts of finding the molecules of interest is complicated. Therefore, for the purpose of identification of molecules altered in a disease state, holistic approaches had to be adopted. Approaches known as "omics" technologies aim at the universal detection of a type of molecules (e.g. genes, transcripts, proteins, metabolites) in an untargeted manner [2] and the term "proteomics" is used to describe the analyses of proteins. Due to the role of proteins in executing biological processes, one of the main scopes of proteomics has become the identification of disease biomarkers [3].

There are two main sources for the identification of disease biomarkers: tissue and body fluids. The advantages of the latter compared to the tissue are: lower invasiveness, less cost, easier sample collection and storage, less demanding sample processing [4]. The applicability of body fluids to study a specific disease should be evaluated with caution and body fluids that have a direct contact with a tissue of interest should be generally taken into consideration. For example, urine is an ideal source to study kidney diseases, however to identify biomarkers for Alzheimer disease, cerebrospinal fluid (CSF) is more applicable [5, 6]. Additionally, body fluids can be very complex and protein concentrations in such samples span over several orders of magnitude. Considering that the potential biomarker can be present at low concentrations, its identification might be challenging, since highly-abundant proteins might mask the presence of low-abundance molecules. Therefore, to overcome the aforementioned obstacle thorough optimization of the analysis protocol is commonly required prior to mass-spectrometry (MS) analysis [3, 4]. It is especially critical for the identification of disease biomarkers for complex diseases such as chronic kidney disease (CKD).

CKD is defined by a progressive loss of kidney function and characterized based on the decrease in the glomerular filtration rate (GFR) or by an increase of the levels of albumin in urine. The disease is classified into five stages based on the GFR rates as follows: i) patients with GFR: > 90 mL/min per 1•73 m² are classified with stage I; ii) with 60–89 mL/min per 1•73 m² with stage 2; iii) 30–59 mL/min per 1•73 m² with stage 3; iv) 15–29 mL/min per 1•73 m² with

stage 4 and v) less than 15 mL/min per 1•73 m² with stage 5 [7]. There are multiple aspects related to the development of CKD including age, obesity, smoking, diabetes mellitus, hypertension or lupus erythematosus [8, 9]. The final outcome of CKD progression is the end-stage renal disease (ESRD). It takes place when the kidneys function shut down or they function at a rate that is not sufficient to support the everyday needs of the body [10].

In clinical practice, CKD is presently diagnosed based on the levels of proteinuria and/or changes in serum creatinine [11]. While microalbuminuria, defined as urine excretion rate between 30–300 mg/24 hours, is currently the best predictor of diabetic nephropathy, it still shows large inter-individual variability, questioning its accuracy [12]. Furthermore, nearly half of the cohort of patients with type 1 diabetes showed early impairment of kidney functions without increased levels of albumin excretion [13], demonstrating the lack of sensitivity of albuminuria as a diagnostic test. The reduction of the eGFR rate is not easily detectable during the early stages of CKD, but rather during late stages. At this point however, the treatment options are already impaired. Based on the literature data, multiple protein biomarkers show potential value in the diagnosis of CKD. Most importantly, cystatin C shows an improved ability to evaluate eGFR levels compared to creatinine and thus, displaying improved association to disease progression. However, the marker can give unreliable results in patients with rapid cell turnover, uncontrolled thyroid disease or patients using corticosteroids [14]. Many of the identified protein biomarkers (e.g. IL-6, CRP, or BNP) did not show yet any added value compared to frequently applied clinical tests and thus, have not been implemented in everyday practice [12]. Unfortunately, prognostic biomarkers for CKD progression are not commercially available. Therefore, both type of biomarkers for early detection and prognosis of the disease, which are able to aid the clinicians to individually adjust the applied therapy to patients needs are required.

Therefore, the presented thesis focuses on the analysis of blood, urine as well as tissue samples for the identification of biomarkers of CKD progression and elucidation of the mechanism of this complex disease using state-of-the-art proteomics approaches. The first part of the thesis focuses on the identification of biomarkers of CKD progression in plasma of patients with different stages of CKD and patients on haemodialysis (**publication 1**). After the analysis of plasma samples, the next goal was the identification of biomarkers in urine. Since proteinuria negatively affects proteomics analysis of urine samples, as the presence of highly-abundant plasma proteins may mask the identification of putative disease biomarkers, I focused on the optimization of the analysis protocol in urine. To reduce the variability related to sample preparation to minimum, we decided to evaluate the applicability of commercially available

depletion kits that specifically remove highly-abundant proteins (**publication 2**). Based on the corresponding results, none of the methods showed an added value for the analysis of urine samples from CKD patients and thus, the decision was made to analyse unfractionated urine samples after comprehensive optimization of the liquid chromatography coupled to mass-spectrometry (LC-MS/MS) running conditions. Identification of prognostic biomarkers of CKD progression in urine involved the analysis of baseline samples from patients classified as non-progressors and progressors based on their annual changes in estimated glomerular filtration rate. This data is yet unpublished, as for now the validation of short listed protein biomarker candidates identified during the discovery phase is still in progress. Nevertheless, obtained data from the discovery set was integrated with the findings from the analysis of tissue samples from CKD patients using Matrix Assisted Laser Desorption/Ionisation Mass-Spectrometry Imaging (MALDI-MSI) (**publication 3**). Noticeably, the same fragment of alpha-1-antitrypsin, which was found up-regulated in the tissue and classified as a biomarker of CKD progression by MALDI-MSI, was also found with higher abundance in the urine of CKD patients classified as progressors. These findings prove the validity of utilizing data integration procedures. Further correlation of the data with other omics data (e.g. miRNA, peptidomics and metabolomics) is in progress in order to increase power of individual observations and coverage of molecular processes involved in CKD progression. This may lead to the discovery of molecular targets for therapeutic intervention.

3. Methods:

3.1. Sample characteristics:

For the identification of CKD biomarkers in plasma, 14 samples from patients with CKD stage 2-3 and 15 patients with CKD stage 5 on haemodialysis for at least 1 year were used for the discovery set. The validation cohort comprised of 8 healthy controls, 8 patients with CKD stage 3, 8 patients with CKD stage 4, 8 patients with CKD stage 5 not on haemodialysis and 8 patients with CKD stage 5 on haemodialysis.

For the evaluation of depletion strategies in urine, two pooled urine samples corresponding to normal and CKD stage 4 were generated. Each of the pooled samples was analysed in 5 technical replicates using 4 different depletion kits. Additionally, unfractionated urine was analysed. A total of 50 samples were analysed.

The MALDI-Imaging tissue study included only primary glomerulonephritis classified as idiopathic (GN) according to clinical criteria. Fresh-frozen biopsies taken from patients, who underwent renal biopsy with a histological diagnosis of focal segmental glomerulosclerosis (FSGS; n=6), IgA Nephropathy (IgAN; n=6) and membranous glomerulonephritis (MGN; n=7), were collected. Normal cortical biopsies (controls, n=4) corresponded to regions of kidney obtained from radical nephrectomy during tumor treatment. Control patients had no history of functional renal disease.

3.2. Sample preparation:

For the identification of CKD biomarkers in plasma, 10 μL of plasma sample was diluted with 90 μL 0.1% sodium dodecylsulphate, 20 mM dithiothreitol and 0.1 M TrisHCl (pH = 7.6). The sample was sonicated at room temperature for 30 min, followed by denaturation at 95° C for 3 min. Samples were subsequently incubated with 50 mM Iodoacetamide at room temperature for 30 min in the dark followed by the addition of ammonium bicarbonate buffer solution (300 μL, 50 mM), applied to NAP-5 column, and eluted with 1 mL of 50 mM ammonium bicarbonate buffer solution. Twenty micrograms of lyophilized trypsin was added to 50 μL of activation buffer solution, and 2 μL of this solution was added to the eluted sample. Trypsin digestion was carried out overnight at a temperature of 37°C. Samples were then lyophilized, stored at 4°C and resuspended in 100 μL HPLC-grade H2O shortly before mass-spectrometry analysis.

In the case of urine analysis, 500 μL urine aliquots (corresponding to a protein content of 29 μg for normal and 437 μg for CKD sample) were subjected to buffer exchange applying buffers compatible with each depletion method according to the respective manufacturer, and concentrated to a final volume of 20 μL, using 3kDa cut-off Amicon Ultra Centrifugal Filter

Units. Such prepared samples were processed with four commercially available kits targeting the depletion of abundant proteins (immuno-based Seppro IgY14 from Sigma Aldrich, immuno-based ProteoPrep from Sigma Aldrich, immuno-based SpinTrap from GE Healthcare and ion-exchange-based ProteoSpin from Norgen Biotek) according to the manufacturers' protocols. In general, each kit targeted from 2 up to 14 different proteins. To assess the reproducibility of each method, five technical replicates of each of the urine samples from healthy controls and from CKD patients per technique were prepared. Urine samples (5 replicates each) prior to or after subjecting to fractionation were processed following the FASP protocol, commonly applied in our laboratory as previously described [15]. Overnight digestion was conducted by adding trypsin solution in ammonium bicarbonate buffer (trypsin to protein ratio: 1:100). The peptide mixture was lyophilized and resuspended in 20 μL (for urine from healthy controls) and 200μL (for urine from CKD patients) of mobile phase A (0.1% formic acid), due to the different protein load of the two samples.

For tissue analysis, from each specimen, two 4 μm thick sections were cut and thaw-mounted on the same conductive Indium Tin Oxide (ITO) glass slide and stabilized for 30 minutes in a conventional dry oven at 85°C. For the identification process, α-cyano-4-hydroxycinnamic acid (7mg/mL in 50%/0.1% v/v acetonitrile/TFA) was deposited onto consecutive sections sectioned from the previously used renal specimens using the ImagePrep automated sprayer. The matrix was removed from the tissue by washing with a 50%/0.1% v/v acetonitrile/TFA solution. The resulting solution was concentrated using a HETO vacuum concentrator for 30 minutes, to a final volume of 20 μL. A volume of 0.8 μL was spotted onto a Ground Steel MALDI Target Plate, allowed to dry, and then followed by an equal volume of 7 mg/ml α-cyano-4-hydroxycinnamic acid.

3.3. Mass-spectrometry analysis

The plasma extracts (5 μL) were analysed by nanoflow LC–MS/MS using an Orbitrap velos FTMS. Elution was performed on an Acclaim PepMap C18 nano column 75 μm × 50 cm, 2 μm, 100 Å with a linear gradient of solvent of solvent A, 0.1% formic acid and acetonitrile (98:2) against solvent B, 0.1% formic acid and acetonitrile (20:80). The gradient was run from at 1% B for 5 min, rising to 25% B after 360 min then on to 65% B after 480 min. The sample was ionized in positive ion mode using a Proxeon nano spray ESI source (Thermo Fisher, Hemel, UK) and analysed in an Orbitrap Velos FTMS (Thermo Finnigan, Bremen, Germany). The MS was operated in a data-dependent mode (top 40) to switch between MS and MS/MS acquisition and parent ions were fragmented by collision-induced dissociation (CID).

For the evaluation of the applicability of depletion strategies in urine, 6µL (corresponding to 30% for normal and 3% for CKD samples of the respective total peptide mixtures) of the prepared peptide mixture were analysed on a Dionex Ultimate 3000 RSLS nano flow system (Dionex, Camberly UK). After loading onto a Dionex 0.1×20 mm 5 µm C18 nano trap column at a flow rate of 5 µl/min in 98% 0.1% formic acid and 2% acetonitrile, sample was eluted onto an Acclaim PepMap C18 nano column 75 µm×50 cm (Dionex, Sunnyvale, CA, USA), 2 µm 100 Å at a flow rate of 0.3 µl/min. The trap and nano flow column were maintained at 35°C. The samples were eluted with a gradient of solvent A: 0.1% formic acid; solvent B: 100% acetonitrile, 0.1% formic acid, starting at 2%B for 10 min, rising to 5%B at 11 min, 15%B at 73 min and 55%B at 95 min. The eluant was ionized using a Proxeon nano spray ESI source operating in positive ion mode into an Orbitrap Velos FTMS (Thermo Finnigan, Bremen, Germany). The resolution of ions in MS1 was 60,000 and 15,000 for HCD MS2. The top 20 multiply charged ions were selected from each scan for MS/MS analysis using the higher-energy collisional dissociation (HCD) at 35% collision energy.

For MALDI- MSI analysis of tissue samples, all mass spectra were acquired in linear positive mode in the mass range of 3000 to 20000 *m/z* using an UltrafleXtreme (Bruker Daltonik GmbH) MALDI-TOF/TOF MS equipped with a Smartbeam laser operating at 2kHz frequency. External calibration was performed using a mixture of standard proteins within the mass range of 5500 to 17000 *m/z* (ProtMix I, Bruker Daltonics). Images were acquired with a laser diameter of 50 µm and a rastering of 50 µm. For MALDI-MS/MS, representative mass spectra were acquired in reflectron positive mode in the mass range of 700 to 4500 *m/z*. Precursor ions were selected and fragmented using the laser-induced dissociation (LID) and LIFT™ technology and an MS/MS spectra obtained from the accumulation of ~100000 laser shots. External calibration was performed using a mixture of standard peptides within the mass range of 750 to 3500 *m/z* (PepMix I, Bruker Daltonics, Germany).

3.4. Histological evaluation.

Following MALDI-MSI analysis of tissue samples, the matrix was removed with increasing concentrations of ethanol (70% and 100%) and the slides were stained using Trichrome. The slides were then converted to digital format using a ScanScope CS digital scanner (Aperio, Park Center Dr., Vista, CA, USA) and pathological glomerular areas of interest (Regions of Interest, ROI) were highlighted by a pathologist, which included all of the glomeruli and regions manifesting in pathological alterations related to the disease. This allowed for the direct overlap of images and the integration of proteomic and pathological information. The study only compared the profiles glomerular tufts while tubulointerstitial features were not

considered for the purpose of the current investigation; specific segmental glomerular areas of fibrosis were included. Globally sclerotic areas were excluded.

3.5 Immunohistochemistry (IHC) with alpha-1-antitrypsin (A1AT) antibody

For tissue samples analysis, in order to confirm the proteomics identification, a further series of formalin-fixed paraffin-embedded (FFPE) renal biopsies taken from patients with IgAN and FSGS were tested for IHC analysis. This validation group included IgAN with wide sclerosis (n=4), IgAN with a prevalent mesangioproliferative pattern without sclerosis (n=4) and FSGS (n=6). For each specimen, 3μm thick sections were cut from FFPE blocks. After deparaffinization and rehydration, slides underwent endogenous peroxidase blockage and an antigen retrieval process via EnVision Flex (DAKO). Finally, Autostainer Link 48 (Dako, Glostrup, Denmark) was used to apply the primary antibody directed against A1AT (polyclonal rabbit, Dako).

3.6. ELISA

To validate the findings in plasma, lysozyme C [Abcam (ab108880)], complement factor D [(R&D Systems (DFD00)], leucine-rich alpha-2-glycoprotein [Cusabio (CSB-E12962 h)] and histidine-rich glycoprotein [Cusabio (CSB-E13159 h)] were quantified by ELISA according to manufacturer's guidelines. Samples were analysed using the EL808 Ultra Microplate Reader using KC4V3.0 Analysis Software.

3.7. Data Analysis

For plasma samples, peptide analysis was performed using SEQUEST against the Human Uniprot Database. Only peptides that showed mass deviation of less than 10 ppm were retained, the peptide data were extracted using high peptide confidence and top one peptide rank filters. The relative quantitative analysis was performed based on the peptide area values. Before analysis, parts per million (ppm)-normalization of peptide areas was conducted, where each of the individual protein peak areas was divided by the sum of peak areas in the sample and multiplied by 10^6. Protein abundance was calculated as the sum of all normalized peptide areas for the given protein. Proteins covered by at least two valid peptides were considered valid.

For urine samples, peptide analysis was performed using SEQUEST against the Human Uniprot Database. Only peptides that showed mass deviation of less than 5 ppm were retained. The peptide data were extracted using high peptide confidence and top five peptide rank filters. The list of peptides was extracted from "Proteome Discoverer" and processed further by an in-house software, where top five rank sequences were harmonized and the most probable sequence per peptide was assigned. Only peptides reported in more than 60% of the samples (3 out of 5

technical replicates) were considered for further evaluation. Protein peak areas were calculated based on the average of top three most abundant peptides for a given protein. Subsequently, normalization of the protein peak areas was conducted based on the modified ppm-normalization method, where depletion targets and putative depletion targets were excluded from calculating total sample peak area (see the original publication for the list of depletion targets and putative depletion targets [15]).

For tissue analysis, flexImaging 3.0 data (Bruker Daltonics, Bremen, Germany), containing spectra of each entire measurement region, were imported into SCiLS Lab 2014 (http://scils.de/; Bremen, Germany) software after the acquisition. SCiLS was used to perform the spectrum analysis. For MALDI-MS/MS spectra, baseline subtraction and smoothing were performed using FlexAnalysis3.4. All MS/MS spectra were searched against the SwissProt database with the Mascot 2.4 search engine. Mass tolerances were set at 2.5-3 Da for MS and 1.4 Da for MS/MS.

3.8. Functional analysis

Differentially expressed proteins from the plasma-based study was subjected to functional analysis using Ingenuity Pathway Analysis software and Cytoscape ClueGo plugin.

3.9. Statistical analysis

For plasma analysis, F-test was performed to test for data distribution. When data were normally distributed, parametric t-test was performed; otherwise, the statistical analysis was performed using Mann–Whitney test or Wilcoxon signed rank test. Multiple hypotheses testing correction was performed using Benjamini–Hochberg test for false discovery rate. Proteins with p-value < 0.05 were considered as statistically significant.

In the case of urine analysis, statistical evaluation was based on the unequal variance 2-tailed Student's t-test. Proteins with p-value ≤ 0.05 and ratio ≥ 1.5 or ≤ 0.66 were considered as statistically significant. Additionally, in the case of relative protein abundance, obtained p-values were adjusted by applying Benjamini-Hochberg correction for multiple testing.

For tissue samples, principal Component Analysis (PCA) was performed to reduce the high complexity of the data. Additionally, Receiver Operative Characteristic (ROC) analysis was performed. Peaks were considered as statistically significant if the AUC was > 0.8 and the p-value < 0.05.

4. Results:

4.1. Publication 1: Glorieux G, Mullen W, Duranton F, Filip S, Gayrard N, Husi H, Schepers E, Neirynck N, Schanstra JP, Jankowski J, Mischak H, Argiles A, Vanholder R, Vlahou A, Klein J. New insights in molecular mechanisms involved in chronic kidney disease using high-resolution plasma proteome analysis. Nephrology, dialysis, transplantation: official publication of the European Dialysis and Transplant Association - European Renal Association. 2015;30(11):1842-52

The plasma samples from 14 patients with CKD stages 2 and 3, and 15 patients on haemodialysis for at least 1 year were analysed by LC-MS/MS. Using label-free approach, we detected 9017 peptides associated with 2054 unique proteins, from which 333 proteins were found as differentially expressed. From these 333 proteins, 206 showed higher abundance and 127 lower abundance in patients on haemodialysis compared to the subjects with CKD 2 and 3. After correction for multiple testing, 39 of the 333 proteins remained significant, where 23 were up-regulated and 16 down-regulated in HD patients compared to CKD 2 and 3 group. For the purpose of this study, we considered all 333 proteins before the correction for multiple testing as statistically significant.

Increased abundance of seven well-characterized uraemic toxins was observed in the obtained dataset [16, 17]. These included cystatin-C, beta-2-microglobulin and prostaglandin-H2 D-isomerase. Increase in their concentrations in plasma showed a significant correlation with renal function decline ($p<0.0001$; rho = -0.57, -0.85 and -0.89 respectively). Two uraemic toxins: immunoglobulins kappa and lambda, were also identified, yet showed similar abundance between compared groups.

Gene Ontology (GO) and Ingenuity Pathway Analysis (IPA) software were used to perform the functional analysis of 333 differentially expressed proteins between compared groups. Several deregulated pathways were identified, including: acute response signalling, complement and coagulation systems, platelet degranulation, calcium ion-dependent exocytosis, atherosclerosis signalling and production of nitric oxide (NO) and reactive oxygen species (ROS) (see original publication for more details [18]).

In the next step of the study we validated the shortlisted protein candidates using ELISA. Additionally, we evaluated if protein concentrations of these shortlisted candidates change during the progression to later stages of CKD. For this purpose plasma samples from patients from an independent cohort comprising of healthy controls, patients with CKD stage 3 (CKD3), CKD stage 4 (CKD4), CKD stage 5 not on HD (CKD5 no HD) and CKD stage 5 on HD (CKD5/HD) (n = 8 per group) were analysed. The cohorts were matched for age and gender.

ELISA analysis confirmed significant increase in complement factor D, lysozyme C and leucine-rich alpha-2 glycoprotein in plasma of CKD5 patients compared with controls. We also demonstrated that the abundance of these three proteins progressively increased during CKD progression to later stages (**Figure 1 A–C**). Moreover, the concentrations of complement factor D and lysozyme C were higher in patients on haemodialysis (CKD5/HD) compared to subjects with CKD 5, but not on haemodialysis (CKD5) (**Figure 2 A–B**). However, changes in histidine-rich glycoprotein abundance observed based on LC-MS/MS analysis were not confirmed by ELISA (**Figure 1 D and Figure 2 D**). In the next step, we evaluated the correlation of plasma concentrations of the proteins with the eGFR levels. In accordance to obtained LC-MS/MS results, complement factor D ($r = -0.9084$, $P < 0.0001$), lysozyme C ($r = -0.7115$, $P < 0.0001$) and leucine-rich alpha-2 glycoprotein ($r = -0.8236$, $P < 0.0001$) were negatively correlated with eGFR. The levels of histidine-rich glycoprotein showed no significant correlation with eGFR.

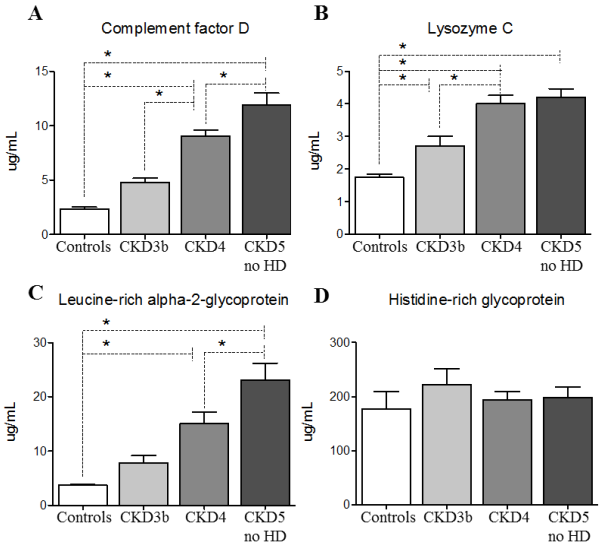

Figure 1. Evaluation of the changes in plasma protein concentrations associated with the progression to later stages of CKD for four tested proteins using ELISA in an independent sample cohort: complement factor D (A), lysozyme C (B), leucine-rich alpha-2-glycoprotein (C) and histidine-rich glycoprotein (D). * denotes $p < 0.05$.

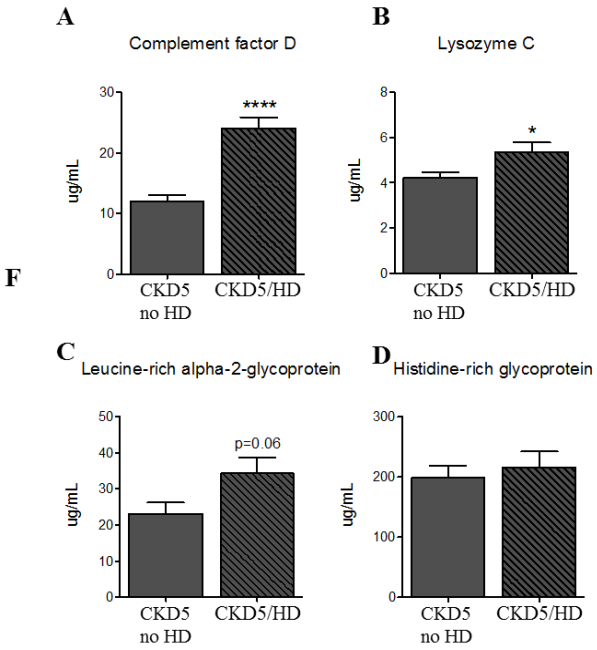

Figure 2 Evaluation of the changes in plasma protein concentrations for four tested proteins between patients with stage 5 CKD not on haemodialysis (CKD5 no HD) and subjects with CKD stage 5 on haemodialysis (CKD5/HD) using ELISA in an independent sample cohort: complement factor D (A), lysozyme C (B), leucine-rich alpha-2-glycoprotein (C) and histidine-rich glycoprotein (D). * denotes $p < 0.05$; **** denotes $p < 0.0001$.

In summary, this study led to the identification of multiple proteins with altered abundance in patients with end stage renal disease compared to subjects with CKD stage 2 and 3 in a relatively large sample cohort using high-resolution mass-spectrometry. The changes in the abundance of complement factor D, lysozyme C and leucine-rich alpha-2-glycoprotein were verified using ELISA in an independent sample cohort, supporting the validity of the proteomics approach. Additionally, the concentrations of these proteins increased with progression to later stages of the disease. In the future, this study may also serve as a basis for investigations concentrating on further evaluation of observed changes.

4.2. Publication 2: Filip S, Vougas K, Zoidakis J, Latosinska A, Mullen W, Spasovski G, Mischak H, Vlahou A, Jankowski J. Comparison of Depletion Strategies for the Enrichment of Low-Abundance Proteins in Urine. PloS one. 2015;10(7):e0133773.

The reproducibility and efficiency of four depletion kits in removing target proteins from urine samples was evaluated. For each of the depletion methods, urine samples from healthy controls and CKD patients were analysed by high-resolution LC-MS/MS in 5 technical replicates. Moreover, to evaluate the efficiency of depletion strategies, unfractionated urine (i.e. initial samples) from healthy controls and CKD patients was also analysed in 5 technical replicates. Therefore, in total 50 samples were analysed in this study. As the main goal of this study was to evaluate the applicability of depletion strategies for the identification of disease biomarkers in urine from large clinical cohorts, where limited urine volumes are usually available, the starting urine volume was established at 500 μL.

After performing the LC-MS/MS analysis, we firstly evaluated the average number of peptides identified in five technical replicates per method. In the case of the urine from healthy controls, unfractionated urine sample showed the highest average number of peptide identifications (approx. 2,400 peptides), followed by ProteoPrep kit (approx. 2150 peptides). Three other kits: ProteoSpin, Seppro IgY14 and SpinTrap kits gave lower number of peptide identifications (approx. 1500 peptides). For the analysis of urine from CKD patients, the number of peptide identifications was comparable between all analysis methods (approx. 1250 peptides in the unfractionated urine and all depleted fractions).

In the next step of the analysis, we concentrated on the number of protein identifications. We specifically focused on proteins identified with high consistency and thus, present in at least three out of five technical replicates per method. Similar number of proteins were detected in unfractionated samples and depleted urine (approx. 390 in healthy controls and 160 in CKD samples). As demonstrated, more proteins were identified in the urine from healthy controls compared to urine from CKD patients, regardless of the analysis method applied. All of the evaluated methods were found to be highly reproducible, since at least 80% of proteins were detected in all five technical replicates.

To assess how the protein depletion affects the relative protein abundance, we evaluated the relative abundance of individual proteins before and after depletion. In **Figure 3** the relative abundance of albumin (as a target protein for all of the kits) and zinc-alpha-2-glycorprotein (as a protein that was not targeted by any of the kits), from undepleted urine (for normal and CKD) was compared to their abundance from corresponding depleted fractions. The application of the evaluated immuno-based methods led to the reduction of relative abundance of the target

proteins for both urine from healthy controls and CKD patients. On the other hand, for the ion-exchange-based kit, the depletion was inefficient for albumin (**Figure 3**) and alpha-1-antitrypsin for CKD as well as serotransferrin in urine from healthy controls. In the case of non-target proteins, no clear trend in the abundance (increase or decrease) was observed, as demonstrated by the example of zinc-alpha-2-glycoprotein (**Figure 3**) (see original publication for more protein examples [15]). Ultimately, protein depletion had an unpredictable effect on protein abundance of non-targeted proteins, questioning any added value of the application of such strategies for the proteomics analysis of urine samples from both healthy controls and CKD patients. Similar results, demonstrating a variable impact of protein depletion were observed in the case of protein sequence coverage (see original publication [15]).

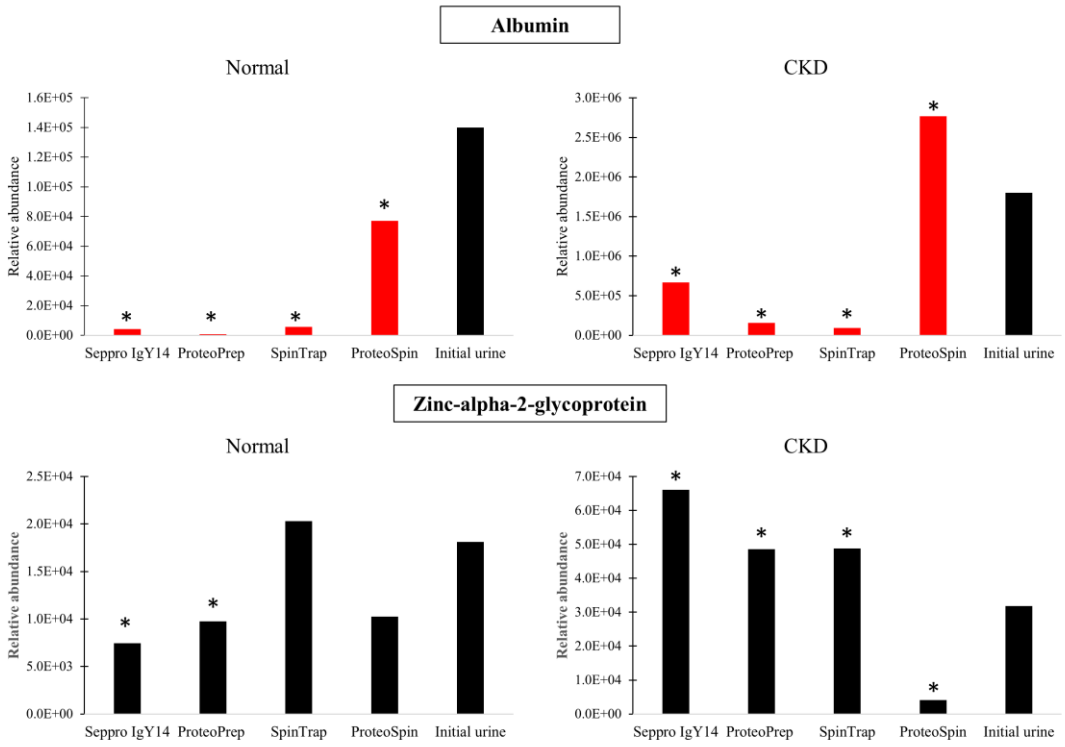

Figure 3. Relative abundance of albumin (as a target protein for all of the depletion kits) and zinc-alpha-2-glycoprotein (as a protein that is not targeted by any of the depletion kits) derived from the LC-MS/MS analysis for unfractionated urine and comparison of their relative abundance with corresponding depleted fractions. Data for healthy controls and CKD patients is shown. Efficient depletion of albumin is observable for all methods, with the exception of ProteoSpin in CKD samples. Red bars indicate that the protein was a depletion target for the evaluated kit. * Denotes statistically significant changes ($p \leq 0.05$) compared to initial (unfractionated) urine.

In summary decrease in the relative abundance of albumin as well other depletion targets following depletion, was typically observed. However, protein depletion did not result in an increase in the number of protein identifications in urine from controls or CKD patients. Therefore, no added value of application of depletion strategies for the proteomics analysis was observed, suggesting that for the identification of CKD biomarkers in urine, the analysis of unfractionated urine samples is preferable.

4.3. Publication 3: Smith A, L'Imperio V, De Sio G, Ferrario F, Scalia C, Dell'Antonio G, Pieruzzi F, Pontillo C, Filip S, Markoska K, Granata A, Spasovski G, Jankowski J, Capasso G, Pagni F, Magni F. alpha-1-antitrypsin detected by MALDI-Imaging in the study of glomerulonephritis: its relevance in chronic kidney disease progression. Proteomics. 2016

In the clinical practice the diagnosis of idiopathic GN, which is associated with CKD progression, is based on the renal biopsy. Nevertheless, tissue biopsy is an invasive procedure associated with some putative complications. Therefore, new diagnostic and prognostic biomarkers that can be translated into less invasive procedures should be identified. This study concentrates on the detection of molecular signatures of glomerulonephritis in tissue. Additionally, it demonstrates the added value of integrating the findings obtained from various sources (i.e. tissue and urinary proteomics) in order to facilitate the detection of putative CKD progression biomarkers. In the future, such findings could be potentially applied in routine diagnosis of idiopathic glomerulonephritis, since due to the invasiveness of the renal biopsy procedure, less-invasive biomarkers are desired.

Fresh frozen renal tissue samples from patients and controls were analysed to detect molecular signatures of primary glomerulonephritis. Signals at *m/z* 4025, 4048 and 4963, demonstrated higher intensities, with a statistical significance ($p < 0.05$ and AUC > 0.8) in patients with primary GN compared to controls. Additionally, patients with FSGS, IgAN and MGN showed several protein signals with altered intensities when compared with each other. From these, the intensities of the signals at *m/z* 4025 and 4048 were significantly increased in patients with FSGS compared to subjects with IgAN and MGN (AUC = 0.84 and 0.82, respectively). Furthermore, in the case of patients with IgAN two signals at *m/z* 4963 and 5072 demonstrated increased intensities compared to FSGS subjects, while signals at *m/z* 5072 and 6180 were higher in IgAN patients in comparison to MGN (see the original publication for more details [19]).

The two signals at *m/z* 4025 and 4048 were able to distinguish sclerotic glomeruli within different forms of primary GN. Thus, to assess their identity, MS/MS spectra of these signals were acquired by MALDI-TOF/TOF. The signal at *m/z* 4048 was identified as a tryptic peptide fragment of α-1-antitrypsin (A1AT) (IPPEVKFNKPFVFLMIEQNTKSPLFMGKVVNPTQK). The immunohistochemistry staining of renal tissue samples for A1AT demonstrated a diffuse positivity within sclerotic areas of FSGS and IgAN and only slight positivity/negativity among IgAN with a prevalent mesangioproliferative pattern and controls. Noticeably, renal biopsies marked as “sclerotic”, showed also strong staining for A1AT in the cytoplasm of podocytes (**Figure 4**). In contrast to the “sclerotic” biopsies, the podocytes present in the renal biopsies

with a mesangioproliferative pattern of IgAN and normal glomeruli were negative for A1AT. This indicates that intraepithelial deposits of A1AT are related to a deregulation of podocytes function. Interestingly, identical tryptic fragment of A1AT was also identified in a different sample cohort with increased abundance in the urine of patients classified as CKD progressors compared to non-progressors (ratio progressors/non-progressors = 5.3, p = 0.02). The agreement between proteomics findings from tissue and urine indicates that A1AT should be investigated as a possible non-invasive biomarker for the prognosis of CKD progression.

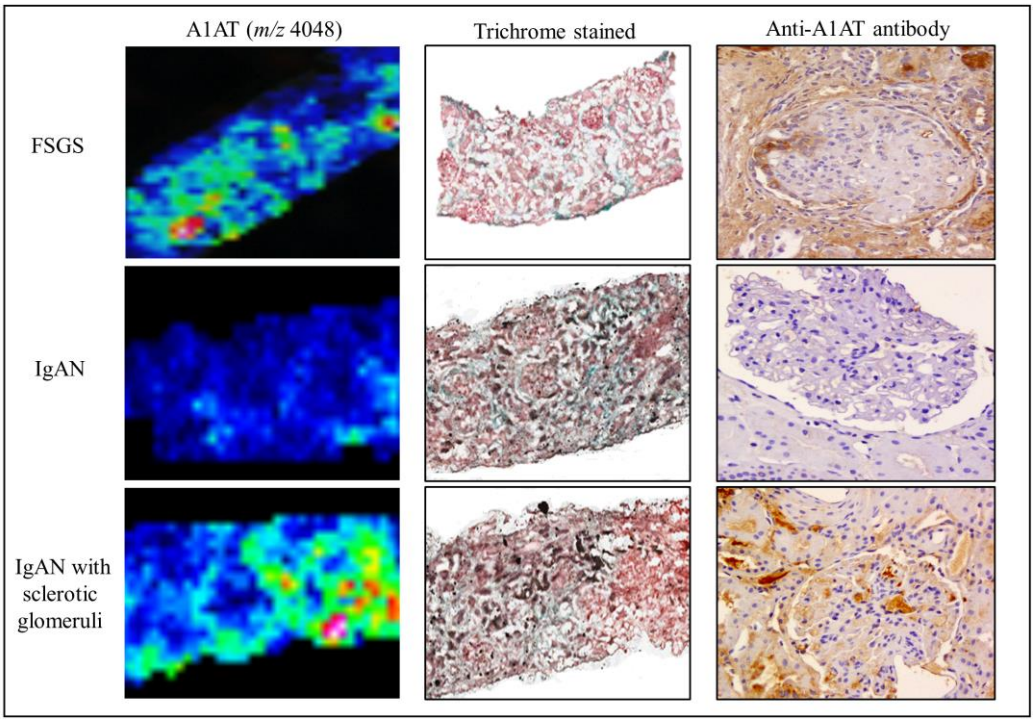

Figure 4. (Left) Distribution of the intensities of the signal identified at m/z 4048 belonging to A1AT acquired by MALDI-MSI; (middle) Trichrome staining of the identical biopsy sections that were used for MALDI-MSI and (right) immunohistochemistry results for A1AT from a validation cohort. The images correspond to the data obtained from patients with FSGS (top), IgAN (middle) and IgAN with sclerotic glomeruli (bottom).

In summary, this study demonstrates a successful application of MALDI-MSI for the identification of putative biomarkers of CKD progression. Additionally, integration of the data from different sources (i.e. tissue biopsy and urinary findings) demonstrates a potential role of the technology to translate results obtained on a tissue level into clinical practice by using easily accessible body fluids.

5. Discussion

CKD is a major public health burden and is associated with a progressive loss of kidney function. Kidney diseases are currently diagnosed by the presence of proteinuria and/or changes in serum creatinine. However, variability between individuals can affect the accuracy of diagnosis [20]. Therefore, novel CKD biomarkers that allow improved detection at early stages and prognosis of disease development need to be identified. To address this issue, the identification of biomarker candidates should be pursued on multiple molecular levels, taking the advantage of integration of the data obtained from different sources. The correlation of the data increases the power of individual observations and coverage of molecular processes involved in CKD progression. This may lead to the discovery of molecular targets for therapeutic intervention. This project aims at the identification of protein biomarkers of CKD progression in plasma, urine (described part focuses on the optimization of the analysis protocol) and tissue samples by using state-of-the-art proteomics approaches. Additionally, integration of the data has taken place and will be expanded in the future.

The aim of the first study [18] was to evaluate the changes in the plasma proteome of patients with the final stage of CKD undergoing haemodialysis compared to those with moderate CKD and detect proteins which levels change with the progression of the disease to late stages. The analysis performed with high-resolution LC-MS/MS led to the identification of 333 proteins differentially expressed between compared groups. Functional analysis of these proteins revealed that many of them are associated with pathways related to acute phase response and complement activation. These findings are in accordance with the literature, since systemic inflammation is a commonly observed aspect in patients with advanced CKD and these on haemodialysis [21, 22]. The increasing levels of three proteins (i.e. complement factor D, lysozyme C and leucine-rich alpha-2-glycoprotein) associated with the progression to late stages of CKD were confirmed by ELISA in an independent sample cohort. From these proteins, increased circulating levels of complement factor D were reported in patients with chronic renal failure and subjects on haemodialysis compared to healthy controls [23]. In this study we demonstrated that the levels of complement factor D progressively increase with the progression to later stages of CKD and even further when the patients are on haemodialysis.

The main goal of the urinary study [15] was to optimize the sample preparation protocol for the proteomics analysis of CKD samples for the identification of CKD progression biomarkers in urine. We therefore evaluated the efficiency of four abundant protein depletion kits (originally designed for plasma) in urine samples from CKD patients and controls. Low-

urine volumes were applied to stimulate conditions typical for large multicentre biomarker studies. Each of the tested methods was reproducible as demonstrated based on the number of peptide and protein identifications. Furthermore, in the case of immuno-based methods all target proteins were efficiently depleted. This observation is not valid for the ion-exchange-based ProteoSpin kit, which was the least efficient in eliminating target proteins from urine samples. Considering the high-specificity of immuno-based mechanism employed in the other kits [24], such situation was expected. Even though in most of the cases the depletion was efficient, the application of depletion strategies did not improve the proteome or sequence coverage. This results are associated with the following reasons: i) complexity of the proteome negatively affects the depletion, resulting in an unpredictable effect on individual proteins; ii) even if enriched, the peptides can still be below the limit of detection for the LC-MS/MS instrument. Ultimately, no significant improvement in the number of identifications, protein sequence coverage or relative abundance in comparison to the unfractionated urine sample was observed. This lack of added value of the application of depletion strategies suggests that for the identification of disease biomarkers in urine, the analysis of unfractionated samples is preferable.

Based on these results, for the identification of CKD progression biomarkers in urine we decided to analyse unfractionated urine samples, after extensive optimization of the LC-MS/MS running conditions. The data is yet unpublished, as we are proceeding with the validation of shortlisted candidates. Still, obtained findings from the discovery set were integrated with the results obtained from the third study [19], focusing on the analysis of tissue samples by MALDI-MSI for the identification of CKD progression biomarkers. MAlDI-MSI was able to distinguish normal kidney from pathological GN, based on specific signals (*m/z* 4025, 4048 and 4963) that were found with higher intensities in the latter compared to controls. These signals may be the indicators of CKD development. Using MALDI-TOF/TOF, the signal at *m/z* 4048 was identified as A1AT, which is an inhibitor of serine proteases. We identified the same tryptic fragment of A1AT to be present with higher abundance in urine of CKD patients classified as progressors compared to non-progressors using the LC-MS/MS analysis. Additionally, urinary naturally occurring peptides that partially overlap with the identified A1AT fragment were previously reported in literature as related to CKD progression by Schanstra *et al*. [11]. Thirty-five urinary fragments of A1AT were found to be associated with disease progression, from which, four fragments partially overlapped with the A1AT fragment identified in tissue by MALDI-MSI. The consistency between tissue and urinary results indicates that A1AT should be further investigated as a putative non-invasive biomarker of CKD progression. Further tests should

concentrate on evaluating both bioptic renal tissue and urine samples from the same patients within a well-defined cohort.

In conclusion, plasma, urine and tissue samples were analysed for the identification of protein biomarkers relative to CKD. In each case thorough optimization of the protocol was performed. Each of these studies brings some new insights regarding the progression of CKD. Furthermore, in order to gain additional information on the pathology of CKD, integration of obtained data was performed. These findings will collectively allow for elucidation of the disease progression mechanism and thus, contribute to the discovery of novel therapeutic targets.

6. References:

[1] Barbosa, EB, Vidotto, A, Polachini, GM, Henrique, T, Marqui, AB, Tajara, EH, Proteomics: methodologies and applications to the study of human diseases. Rev Assoc Med Bras 2012, 58, 366-75.

[2] Horgan, RP, Kenny, LC, 'Omic' technologies: genomics, transcriptomics, proteomics and metabolomics. The Obstetrician & Gynaecologist 2011, 13, 189-95.

[3] Filip, S, Zoidakis, J, Vlahou, A, Mischak, H, Advances in urinary proteome analysis and applications in systems biology. Bioanalysis 2014, 6, 2549-69.

[4] Hu, S, Loo, JA, Wong, DT, Human body fluid proteome analysis. Proteomics 2006, 6, 6326-53.

[5] Lygirou, V, Makridakis, M, Vlahou, A, Biological sample collection for clinical proteomics: existing SOPs. Methods Mol Biol 2015, 1243, 3-27.

[6] Kroksveen, AC, Opsahl, JA, Aye, TT, Ulvik, RJ, Berven, FS, Proteomics of human cerebrospinal fluid: discovery and verification of biomarker candidates in neurodegenerative diseases using quantitative proteomics. J Proteomics 2011, 74, 371-88.

[7] Levey, AS, Coresh, J, Chronic kidney disease. Lancet 2012, 379, 165-80.

[8] Tesauro, M, Mascali, A, Franzese, O, Cipriani, S, Cardillo, C, Di, DN, Chronic kidney disease, obesity, and hypertension: the role of leptin and adiponectin. Int.J.Hypertens. 2012, 2012, 943605.

[9] O'Seaghdha, CM, Lyass, A, Massaro, JM, Meigs, JB, Coresh, J, D'Agostino, RB, Sr., Astor, BC, Fox, CS, A risk score for chronic kidney disease in the general population. Am.J.Med. 2012, 125, 270-7.

[10] Brosnahan, G, Fraer, M, Chronic kidney disease: whom to screen and how to treat, part 1: definition, epidemiology, and laboratory testing. South.Med.J. 2010, 103, 140-6.

[11] Schanstra, JP, Zurbig, P, Alkhalaf, A, Argiles, A, Bakker, SJ, Beige, J, Bilo, HJ, Chatzikyrkou, C, Dakna, M, Dawson, J, Delles, C, Haller, H, Haubitz, M, Husi, H, Jankowski, J, Jerums, G, Kleefstra, N, Kuznetsova, T, Maahs, DM, Menne, J, Mullen, W, Ortiz, A, Persson, F, Rossing, P, Ruggenenti, P, Rychlik, I, Serra, AL, Siwy, J, Snell-Bergeon, J, Spasovski, G, Staessen, JA, Vlahou, A, Mischak, H, Vanholder, R, Diagnosis and Prediction of CKD Progression by Assessment of Urinary Peptides. J Am Soc Nephrol 2015, 26, 1999-2010.

[12] Filip, S, Pontillo, C, Peter Schanstra, J, Vlahou, A, Mischak, H, Klein, J, Urinary proteomics and molecular determinants of chronic kidney disease: possible link to proteases. Expert Rev Proteomics 2014, 11, 535-48.

[13] Perkins, BA, Ficociello, LH, Roshan, B, Warram, JH, Krolewski, AS, In patients with type 1 diabetes and new-onset microalbuminuria the development of advanced chronic kidney disease may not require progression to proteinuria. Kidney Int 2010, 77, 57-64.
[14] Shlipak, MG, Mattes, MD, Peralta, CA, Update on cystatin C: incorporation into clinical practice. Am J Kidney Dis 2013, 62, 595-603.
[15] Filip, S, Vougas, K, Zoidakis, J, Latosinska, A, Mullen, W, Spasovski, G, Mischak, H, Vlahou, A, Jankowski, J, Comparison of Depletion Strategies for the Enrichment of Low-Abundance Proteins in Urine. PLoS One 2015, 10, e0133773.
[16] Duranton, F, Cohen, G, De Smet, R, Rodriguez, M, Jankowski, J, Vanholder, R, Argiles, A, European Uremic Toxin Work, G, Normal and pathologic concentrations of uremic toxins. J Am Soc Nephrol 2012, 23, 1258-70.
[17] Vanholder, R, De Smet, R, Glorieux, G, Argiles, A, Baurmeister, U, Brunet, P, Clark, W, Cohen, G, De Deyn, PP, Deppisch, R, Descamps-Latscha, B, Henle, T, Jorres, A, Lemke, HD, Massy, ZA, Passlick-Deetjen, J, Rodriguez, M, Stegmayr, B, Stenvinkel, P, Tetta, C, Wanner, C, Zidek, W, European Uremic Toxin Work, G, Review on uremic toxins: classification, concentration, and interindividual variability. Kidney Int 2003, 63, 1934-43.
[18] Glorieux, G, Mullen, W, Duranton, F, Filip, S, Gayrard, N, Husi, H, Schepers, E, Neirynck, N, Schanstra, JP, Jankowski, J, Mischak, H, Argiles, A, Vanholder, R, Vlahou, A, Klein, J, New insights in molecular mechanisms involved in chronic kidney disease using high-resolution plasma proteome analysis. Nephrol Dial Transplant 2015, 30, 1842-52.
[19] Smith A, L'Imperio V, De Sio G, Ferrario F, Scalia C, Dell'Antonio G, Pieruzzi F, Pontillo C, Filip S, Markoska K, Granata A, Spasovski G, Jankowski J, Capasso G, Pagni F, Magni F. alpha-1-Antitrypsin detected by MALDI imaging in the study of glomerulonephritis: Its relevance in chronic kidney disease progression. Proteomics 2016;16(11-12):1759-66.
[20] Pejcic, M, Stojnev, S, Stefanovic, V, Urinary proteomics--a tool for biomarker discovery. Ren Fail 2010, 32, 259-68.
[21] Romao, JE, Jr., Haiashi, AR, Elias, RM, Luders, C, Ferraboli, R, Castro, MC, Abensur, H, Positive acute-phase inflammatory markers in different stages of chronic kidney disease. Am J Nephrol 2006, 26, 59-66.
[22] Schoorl, M, Grooteman, MP, Bartels, PC, Nube, MJ, Aspects of platelet disturbances in haemodialysis patients. Clin Kidney J 2013, 6, 266-71.
[23] Volanakis, JE, Barnum, SR, Giddens, M, Galla, JH, Renal filtration and catabolism of complement protein D. N Engl J Med 1985, 312, 395-9.

[24] Moser, AC, Hage, DS, Immunoaffinity chromatography: an introduction to applications and recent developments. Bioanalysis 2010, 2, 769-90.

7. Appendix

7.1. Affidavit

I, Szymon Filip certify under penalty of perjury by my own signature that I have submitted the thesis on the topic “Identification of protein biomarkers for chronic kidney disease progression using state-of-the-art proteomics approaches”. I wrote this thesis independently and without assistance from third parties, I used no other aids than the listed sources and resources.

All points based literally or in spirit on publications or presentations of other authors are, as such, in proper citations (see "uniform requirements for manuscripts (URM)" the ICMJE www.icmje.org) indicated. The sections on methodology (in particular practical work, laboratory requirements, statistical processing) and results (in particular images, graphics and tables) correspond to the URM (s.o) and are answered by me. My contributions in the selected publications for this dissertation correspond to those that are specified in the following joint declaration with the responsible person and supervisor. All publications resulting from this thesis and which I am author of correspond to the URM (see above) and I am solely responsible.

The importance of this affidavit and the criminal consequences of a false affidavit (section 156,161 of the Criminal Code) are known to me and I understand the rights and responsibilities stated therein.

_____

Date Signature

7.2. Statement of originality

Szymon Filip had the following share in the following publications:

Publication 1: Glorieux G, Mullen W, Duranton F, Filip S, Gayrard N, Husi H, Schepers E, Neirynck N, Schanstra JP, Jankowski J, Mischak H, Argiles A, Vanholder R, Vlahou A, Klein J. New insights in molecular mechanisms involved in chronic kidney disease using high-resolution plasma proteome analysis. Nephrology, dialysis, transplantation: official publication of the European Dialysis and Transplant Association - European Renal Association, 2015.

Contribution in detail: participation in data and pathway analysis, critical evaluation of the manuscript and acceptance of the final version.

Publication 2: Filip S, Vougas K, Zoidakis J, Latosinska A, Mullen W, Spasovski G, Mischak H, Vlahou A, Jankowski J. Comparison of Depletion Strategies for the Enrichment of Low-Abundance Proteins in Urine. PloS one, 2015.

Contribution in detail: sample preparation, data processing, data analysis, statistical analysis and writing of the manuscript.

Publication 3: Smith A, L'Imperio V, De Sio G, Ferrario F, Scalia C, Dell'Antonio G, Pieruzzi F, Pontillo C, Filip S, Markoska K, Granata A, Spasovski G, Jankowski J, Capasso G, Pagni F, Magni F. alpha-1-antitrypsin detected by MALDI-Imaging in the study of glomerulonephritis: its relevance in chronic kidney disease progression. Proteomics, 2016.

Contribution in detail: integration of MALDI findings (data) with urinary proteomics data, critical evaluation of the manuscript and acceptance of the final version.

Signature, date and stamp of the supervising University teacher

_____

Signature of the doctoral candidate

_____

7.3 Selected publications

Publication 1: Glorieux G, Mullen W, Duranton F, Filip S, Gayrard N, Husi H, Schepers E, Neirynck N, Schanstra JP, Jankowski J, Mischak H, Argiles A, Vanholder R, Vlahou A, Klein J. New insights in molecular mechanisms involved in chronic kidney disease using high-resolution plasma proteome analysis. Nephrology, dialysis, transplantation: official publication of the European Dialysis and Transplant Association - European Renal Association, 2015;30(11):1842-52. Excluded article. Full text link: http://dx.doi.org/10.1093/ndt/gfv254.

Publication 2: Filip S, Vougas K, Zoidakis J, Latosinska A, Mullen W, Spasovski G, Mischak H, Vlahou A, Jankowski J. Comparison of Depletion Strategies for the Enrichment of Low-Abundance Proteins in Urine. PloS one, 2015;10(7):e0133773. Open access.

Publication 3: Smith A, L'Imperio V, De Sio G, Ferrario F, Scalia C, Dell'Antonio G, Pieruzzi F, Pontillo C, Filip S, Markoska K, Granata A, Spasovski G, Jankowski J, Capasso G, Pagni F, Magni F. alpha-1-Antitrypsin detected by MALDI imaging in the study of glomerulonephritis: Its relevance in chronic kidney disease progression. Proteomics, 2016;16(11-12):1759-66.

PLOS ONE

RESEARCH ARTICLE

Comparison of Depletion Strategies for the Enrichment of Low-Abundance Proteins in Urine

Szymon Filip[1,2], Konstantinos Vougas[1], Jerome Zoidakis[1], Agnieszka Latosinska[1,2], William Mullen[3], Goce Spasovski[4], Harald Mischak[3,5], Antonia Vlahou[1], Joachim Jankowski[6]*

1 Biomedical Research Foundation Academy of Athens, Biotechnology Division, Athens, Greece, **2** Charité–Universitätsmedizin Berlin, Berlin, Germany, **3** University of Glasgow Institute of Cardiovascular and Medical Sciences, Glasgow, United Kingdom, **4** Ss. Cyril and Methodius University in Skopje, Nephrology Department, Skopje, Former Yugoslav Republic of Macedonia, **5** Mosaiques Diagnostics GmbH, Hannover, Germany, **6** University Hospital RWTH Aachen, Institute for Molecular Cardiovascular Research, Aachen, Germany

* jjankowski@ukaachen.de

Citation: Filip S, Vougas K, Zoidakis J, Latosinska A, Mullen W, Spasovski G, et al. (2015) Comparison of Depletion Strategies for the Enrichment of Low-Abundance Proteins in Urine. PLoS ONE 10(7): e0133773. doi:10.1371/journal.pone.0133773

Editor: Lennart Martens, UGent / VIB, BELGIUM

Received: March 9, 2015

Accepted: July 1, 2015

Published: July 24, 2015

Data Availability Statement: All relevant data are within the paper and its Supporting Information files.

Funding: The research presented in this manuscript was supported by "Clinical and system -omics for the identification of the Molecular Determinants of established Chronic Kidney Disease (iMODE-CKD, PEOPLE-ITN-GA-2013-608332). The funders had no role in study design, data collection and analysis, decision to publish, or preparation of the manuscript.

Competing Interests: Mosaiques Diagnostics GmbH provided support in the form of salaries for authors (HM), but did not have any additional role in the study design, data collection and analysis,

Abstract

Proteome analysis of complex biological samples for biomarker identification remains challenging, among others due to the extended range of protein concentrations. High-abundance proteins like albumin or IgG of plasma and urine, may interfere with the detection of potential disease biomarkers. Currently, several options are available for the depletion of abundant proteins in plasma. However, the applicability of these methods in urine has not been thoroughly investigated. In this study, we compared different, commercially available immunodepletion and ion-exchange based approaches on urine samples from both healthy subjects and CKD patients, for their reproducibility and efficiency in protein depletion. A starting urine volume of 500 μL was used to simulate conditions of a multi-institutional biomarker discovery study. All depletion approaches showed satisfactory reproducibility (n=5) in protein identification as well as protein abundance. Comparison of the depletion efficiency between the unfractionated and fractionated samples and the different depletion strategies, showed efficient depletion in all cases, with the exception of the ion-exchange kit. The depletion efficiency was found slightly higher in normal than in CKD samples and normal samples yielded more protein identifications than CKD samples when using both initial as well as corresponding depleted fractions. Along these lines, decrease in the amount of albumin and other targets as applicable, following depletion, was observed. Nevertheless, these depletion strategies did not yield a higher number of identifications in neither the urine from normal nor CKD patients. Collectively, when analyzing urine in the context of CKD biomarker identification, no added value of depletion strategies can be observed and analysis of unfractionated starting urine appears to be preferable.

decision to publish, or preparation of the manuscript. The specific roles of these authors are articulated in the 'author contributions' section.

Introduction

Advances in mass spectrometry (MS) have recently facilitated the development of high-throughput and sensitive analysis methods for proteomics investigations [1–3]. However, proteome analysis of complex biological samples remains challenging, among others due to the huge abundance differences among individual protein components; for example, in plasma, the presence of albumin or immunoglobulins (IgG) and other predominant proteins hinder the detection of less abundant proteins and reduces the efficiency of LC-MS/MS analysis [4]. This masking effect is also expected to be pronounced in the analysis of the urinary proteome of patients with chronic kidney disease (CKD) who present high levels of urinary albumin [5]. Furthermore, albumin abundance is highly variable between patients with CKD, even with the same disease etiology, which further complicates the analysis and comparison of the urinary protein content of these samples [6, 7]. Similarly to plasma [8], the range of protein concentration in urine spans several orders of magnitude [9, 10]. Due to the fact that the concentration of potential disease biomarkers might be relatively low, predominant proteins may mask them and make their identification challenging. Therefore, fractionation and depletion strategies are generally employed prior to MS analysis [11].

Currently, several fractionation methods for protein depletion are available. Some of them are based on the separation of proteins by physicochemical properties such as charge (ion-exchange [12]) or size (size-exclusion chromatography [13]), while others target specific protein groups or ligands, such as glycosyl groups in the case of glycoproteins [14] or biochemical properties (i.e. immunoaffinity [15]). These affinity chromatography methods are applicable for a rapid and selective depletion or enrichment of biomolecules from complex samples [16, 17]. The selection of a fractionation strategy depends on the specific study requirements. For example, combinatorial peptide ligand libraries, allow for the simultaneous depletion of highly-abundant proteins and enrichment of low-abundance targets, facilitating their detection by MS [18]. However, this approach requires relatively high amounts of starting material (hundreds of milliliters of urine) to ensure efficient enrichment of low-abundance proteins; otherwise, high- and medium-abundance proteins would not fully saturate their ligands and ultimately the elution would have the same profile as initial sample [19–21]. Since in most cases low volumes of urine (<1 mL) are available when investigating prospectively collected samples from clinical cohorts, combinatorial ligand peptide libraries do not appear to be applicable for analysis of such individual urine samples. [21]. Strategies based on the depletion of abundant proteins require lower initial material compared to combinatorial peptide ligand libraries [21, 22]. These strategies include immuno-based depletion methods involving selective binding of target proteins to the stationary phase based on affinity. They are considered to have high specificity and efficiency and achieve rapid purification or concentration of the analytes [15]. Another depletion strategy is based on ion-exchange chromatography relying on attraction of oppositely charged molecules as the basis for separation [12].

Depletion of abundant proteins appears especially relevant when investigating the urinary proteome of CKD patients, where the levels and variability of highly-abundant proteins noticeably increase with each stage of CKD [5]. On the other hand, depletion of abundant proteins causes co-depletion of several low-abundance proteins, hindering their detection [23–25]. Several protein depletion kits are commercially available. These kits are generally designated to be used for plasma samples and their application has been evaluated in several manuscripts (e.g. [22, 24, 26–28]). Kulloli et al. [28] applied a kit for depletion of 14 abundant proteins in plasma prior to analysis by LC-MS/MS. The depletion allowed to enrich the sample for low-abundance proteins and increased the number of identifications compared to the non-depleted sample (from approx. 71 to 130 proteins). Similarly, Tu et al. [26] observed a 25% increase in the

number of identifications when kits depleting 7 or 14 high-abundance proteins were applied prior to the LC-MS/MS analysis. However, the authors questioned the applicability of the depletion strategy for the identification of disease biomarkers in plasma, since the low-abundance proteins accounted only for 6% of total identifications and 50 of the proteins with the highest abundance accounted for 90% of total spectral counts. Along the same lines, two-dimensional gel electrophoresis (2DE) analyses of plasma samples, where depletion of abundant proteins strategy was applied, demonstrated an increase in the number of spots on the gel. Yet, most of the newly identified spots, represented different isoforms of high-abundance proteins (e.g. albumin, IgGs) [24, 27].

Various protein depletion kits have been also tested on urine samples [29–32]. Afkarian et al. [31] depleted albumin and IgG from urine of diabetic patients with or without nephropathy. Subsequently, iTRAQ labeling was performed and the samples were analyzed by 2D-LC-MS (MALDI-TOF/TOF). No increase in the number of identified proteins was observed in the depleted samples, regardless if the patient was normo- or macro-albuminuric. On the other hand, Kushnir et al. [30] reported a 2.5-fold increase in the number of protein identifications by LC-MS/MS after depleting 6 highly abundant proteins (albumin, IgG, alpha-1 antitrypsin, IgA, transferring and haptoglobin) using multiple affinity removal (MARS) column (Agilent Technologies, Santa Clara, CA). Abundant protein depletion strategies (14 MARS) in conjunction with iTRAQ labeling were also applied for the identification of potential bladder cancer biomarkers from urine [33]. The depletion strategy allowed increasing the number of identifications from approximately 300 proteins in the non-fractionated sample to 500, and the discovery of a potential biomarker panel for bladder cancer [33].

Collectively, based on the existing conflicting data it is presently unclear whether depletion strategies are of benefit when analyzing urine samples. In this study, we therefore aimed to assess the effectiveness of different commercially available depletion strategies for the proteome analysis of urine samples from CKD patients and healthy controls: four different strategies (three immunodepletion- and one ion-exchange-based) were applied prior to LC-MS/MS analysis. The efficiency of depletion, reproducibility, and the overall impact of each strategy on the number of protein identifications and relative protein quantification were assessed.

Materials and Methods

Sample characteristics

Second morning mid-stream urine samples were employed. To remove cell debris, urine was centrifuged at 1,000xg for 10 min at 4°C. Two pooled urine samples (with a final volume of approx. 30 mL each) corresponding, to normal and CKD (stage IV) were generated. Protein content was estimated by Bradford protein assay. To reduce freeze-thaw cycles to minimum, samples were aliquoted in 500 μL (40 aliquots per CKD and normal pool) and kept at -20°C until used. Sample collection was performed in accordance to local ethics requirements and the study was approved by the local ethics committee ("Macedonia Academy of Sciences and Arts"; ethics subcommittee for medicine, pharmacy, veterinary and stomatology: 07–65711, 1-04-2013). All individuals gave written informed consent.

Chromatography approaches

500 μL urine aliquots (corresponding to a protein content of 29 μg for normal and 437 μg for CKD sample) were subjected to buffer exchange applying buffers compatible with each depletion method according to the respective manufacturer, and concentrated to a final volume of 20 μL, using Amicon Ultra Centrifugal Filter Units (3kDa cut-off, Millipore).

Table 1. Characteristics of the applied depletion strategies.

Depletion kit	Company	Mechanism	Depleted proteins
Seppro IgY14	Sigma Aldrich	Immunodepletion	Albumin, IgG, α1-Antitrypsin, IgA, IgM, Transferrin, Haptoglobin, α2-Macroglobulin, Fibrinogen, Complement C3, α1-Acid Glycoprotein (Orosomucoid), HDL (Apolipoproteins A-I and A-II), LDL (mainly Apolipoprotein B)
ProteoPrep	Sigma Aldrich	Immunodepletion	Albumin, IgG
SpinTrap	GE Healthcare	Immunodepletion	Albumin, IgG
ProteoSpin	Norgen Biotek	Ion-exchange	Albumin, alpha-1-antitrypsin, transferrin and haptoglobin

doi:10.1371/journal.pone.0133773.t001

Such prepared samples were processed with four commercially available kits targeting the depletion of abundant proteins (Table 1) according to the manufacturers' protocols. To assess the reproducibility of each method, five technical replicates of each of the urine samples from healthy controls and from CKD patients per technique were prepared. Depleted samples were obtained either from the flow-through fraction for three immuno-based kits: Seppro IgY14 (Sigma-Aldrich, Saint Louis, MO, USA), ProteoPrep (Sigma-Aldrich, Saint Louis, MO, USA) and SpinTrap (GE Healthcare, Little Chalfont, UK) or in the elution fraction for the ion-exchange kit: ProteoSpin (Norgen Biotek, Thorold, Canada). Protein content after depletion was quantified by Bradford protein assay. The protocol for each depletion kit is briefly described below:

Seppro IgY14: (loading capacity: up to 1000 μg of total protein content) After buffer exchange to "Dilution Buffer" (100 mM Tris-Buffered Saline, Tris-HCl with 1.5 M NaCl, pH 7.4) and concentration to 20 μL, urine sample was further diluted with the "Dilution Buffer" to a final volume of 500 μL. Depletion column was centrifuged to remove the storage buffer and the sample was applied to the column. In brief, the sample was thoroughly mixed with the column resin and incubated on an end-to-end rotator for 15 minutes. This step ensures binding of target proteins to the resin. Afterwards, the sample was centrifuged and the first depleted fraction was collected. Subsequently, to increase the recovery rate of proteins not binding to the resin, 500 μL of "Dilution Buffer" was added onto the column and centrifuged once more. Two fractions (0.5 mL each), corresponding to depleted sample, were combined prior to filter-aided sample preparation (FASP) for LC-MS/MS analysis. The depleted sample was analyzed by SDS-PAGE and LC-MS/MS. To prepare the column for another use, bound proteins were stripped off the column resin by applying "Elution Buffer" (1 M glycine, pH 2.5) followed by 3 min incubation, according to the manufacturer's instructions. Afterwards, the column resin was rinsed and kept in the storage buffer until further use.

ProteoPrep: (loading capacity: up to 3000 μg of total protein content) After buffer-exchange to "Equilibration Buffer" (low ionic strength Tris buffer, pH 7.4) and concentration to 20 μL, the sample was further diluted with "Equilibration Buffer" to a final volume of 100 μL. Diluted sample was then loaded onto the equilibrated column (prepared according to the manufacturer's instructions) and incubated for 10 minutes to allow binding of the target proteins to the column resin. This step was repeated once. The sample was centrifuged and in order to collect remaining unbound proteins, 125 μL of "Equilibration Buffer" was added onto the column. The depleted sample comprised of the flow-through from previous step and the wash (in total 225 μL). The depleted sample was analyzed by both SDS-PAGE and LC-MS/MS. To collect bound proteins for analysis by SDS-PAGE, the column was eluted twice with 150 μL of "Protein Extraction Reagent" (40 mM Trizma Base, 7.0 M urea, 2.0 M thiourea and 1% C_7BzO detergent, pH 10.4). Elution fraction was also kept for further analysis by SDS-PAGE.

SpinTrap: (loading capacity: up to 3000 μg of total protein content) After buffer-exchange to "Binding Buffer" (20 mM sodium phosphate, 0.15 M sodium chloride, pH 7.4) and concentration to 20 μL, the sample was diluted with the Binding Buffer to a final volume of 100 μL. The column was equilibrated, the sample was applied onto the column and incubated for 5 min. Unbound sample components were collected by centrifugation, and the column was washed twice with 100 μL of "Binding Buffer". The depleted sample comprised of these three collected fractions (flow-through of the loaded sample and two washes—300 μL) and was further analyzed by SDS-PAGE and LC-MS/MS. Bound proteins were eluted by adding 150 μL of "Elution Buffer" (0.1 M glycin-HCl, pH 2.7) twice. These obtained fractions (300 μL) were also combined and further analyzed by SDS-PAGE.

ProteoSpin: (loading capacity: up to 500 μg of total protein content) After buffer-exchange to "Binding Buffer" (20 mM sodium phosphate, 0.15 M sodium chloride, pH 7.4) and concentration to 20 μL, the sample was diluted with the "Column Activation and Wash Buffer" (composition not specified by the manufacturer) to a final volume of 500 μL. The column was activated followed by application of the diluted sample. During this step, the non-targeted proteins bind to the resin. Afterwards, the samples were centrifuged. The flow-through containing the highly-abundant target proteins was kept for SDS-PAGE analysis. The column was then washed twice with 500 μL of "Column Activation and Wash Buffer". 100 μL of the "Elution Buffer" (composition not specified by the manufacturer) was added and the column was centrifuged. This step was repeated twice. Collected fractions (200 μL) were combined. This depleted sample was analyzed by SDS-PAGE and LC-MS/MS.

1-dimensional gel electrophoresis (SDS-PAGE)

15μL of each chromatography fraction were loaded on a 10% acrylamide gel and SDS-PAGE was performed. The gels were stained with silver [34].

Sample preparation for LC-MS/MS

Urine samples (5 replicates each) prior to or after subjecting to fractionation (Table 1) were processed following the FASP protocol, commonly applied in our laboratory as described previously [35], with minor modifications. Specifically, in brief, samples were concentrated to a final volume of 50 μL using Amicon Ultra Centrifugal Filter Units (30kDa cut-off, Millipore, Billerica, MA, USA) at 13,000 rpm and incubated with 0.1 M 1,4-Dithioerythritol for 20 min. Subsequently, two centrifugal wash steps were performed by adding 200 μL urea buffer (8M urea in 0.1M TRIS-HCl, pH 8.5). After these centrifugation steps, protein alkylation was conducted by adding 100 μL of iodoacetamide solution (0.05M iodoacetamide in urea buffer) and incubating the mixture for 20 min in the dark. Afterwards, two additional washes with urea buffer were performed followed by two washes with ammonium bicarbonate (ABC) buffer (50mM NH_4HCO_3, pH 8). Overnight digestion was conducted by adding trypsin solution in ABC buffer (trypsin to protein ratio—1:100). Peptides were eluted by centrifugation followed by filter washing with 40 μL ABC solution. The peptide mixture was lyophilized and resuspended in 20 μL (for urine from healthy controls) and 200μL (for urine from CKD patients) of mobile phase A (0.1% formic acid), due to the different protein load of the two samples.

LC-MS/MS analysis

6μL (corresponding to 30% for normal and 3% for CKD samples of the respective total peptide mixtures) of the prepared peptide mixture were analyzed on a Dionex Ultimate 3000 RSLS nano flow system (Dionex, Camberly UK). After loading onto a Dionex 0.1×20 mm 5 μm C18 nano trap column at a flow rate of 5 μl/min in 98% 0.1% formic acid and 2% acetonitrile,

sample was eluted onto an Acclaim PepMap C18 nano column 75 μm×50 cm (Dionex, Sunnyvale, CA, USA), 2 μm 100 Å at a flow rate of 0.3 μl/min. The trap and nano flow column were maintained at 35°C. The samples were eluted with a gradient of solvent A: 0.1% formic acid; solvent B: 100% acetonitrile, 0.1% formic acid, starting at 2%B for 10 min, rising to 5%B at 11 min, 15%B at 73 min and 55%B at 95 min. The column was then washed and re-equilibrated prior to injection of the next sample.

The eluant was ionized using a Proxeon nano spray ESI source operating in positive ion mode into an Orbitrap Velos FTMS (Thermo Finnigan, Bremen, Germany). Ionization voltage was 2.2 kV and the capillary temperature was 250°C. The mass-spectrometer was operated in MS/MS mode scanning from 350 to 2,000 amu. The resolution of ions in MS1 was 60,000 and 15,000 for HCD MS2. The top 20 multiply charged ions were selected from each scan for MS/MS analysis using HCD at 35% collision energy.

Protein identification and data processing

Protein identification was performed using the SEQUEST search engine (Proteome Discoverer 1.4, Thermo Scientific). Protein search was performed against the SwissProt human protein database (30.10.2013) containing 20277 entries without protein isoforms. The following search parameters were applied: i) fragment mass tolerance: 0.05Da; ii) full tryptic digestion; iii) max missed cleavage sites: 2; iv) static modifications: carbamidomethylation of cysteine; v) dynamic modifications: oxidation of methionine; vi) event detector mass precision: 2 ppm; vii) min. precursor mass: 600 Da; viii) max. precursor mass: 5000 Da; ix) min. collision energy: 0 eV; x) max. collision energy 100 eV; xi) target FDR (strict): 0.01; xii) target FDR (relaxed): 0.05; xiii) FDR validation based on: q-Value. Obtained results were further processed by applying the following filters: i) high confidence (FDR <1%); ii) mass peak deviation: 5 ppm; iii) at least one unique peptide per protein; iv) peptide and protein grouping were enabled. Additionally, since the same peptide can be associated with two (or more) different sequences in different experiments and hence be "lost" for comparison, we initially collected information on the top5 ranked sequences. In the next steps using an in-house developed software (described in the next paragraph), these sequences were harmonized so that the most probable sequence per peptide is assigned, improving the data consistency.

Specifically, the list of peptides was exported from "Proteome Discoverer" and processed further as follows; For each spectrum, the corresponding sequence was defined based on the relative number of sequence identifications in each sample. The relative quantitative analysis was performed based on the peptide area values. Obtained sequences for all technical replicates were merged. Peptides were assigned to the corresponding proteins after merging the list of peptides from 5 technical replicates. Peptides corresponding to multiple proteins were assigned to the protein identified based on the highest number of peptides ("Occam's Razor rule" [36]). Due to a bug in "Proteome Discoverer", for a limited number of peptide identifications the area was not retrieved. If such situation occurred, missing values were replaced by the mean area for the group. Only peptides reported in more than 60% of the samples (3 out of 5 technical replicates) were considered for the calculations of the number of peptide and protein identifications, protein peak areas, sequence coverage, evaluation of consistency and statistical analysis.

Protein peak area was calculated based on the average of top three most abundant peptides for a given protein. Subsequently, normalization of the protein peak areas was conducted. Depletion targets and putative targets were excluded from calculating total sample peak area, since levels of these proteins change between each method applied, introducing bias and falsely increasing the abundance of other proteins. Therefore, the data were normalized based on non-target proteins, which, in principle, should remain unchanged. The validity of this method

was confirmed following a comparison of normalized values to ELISA measurements of albumin (data not shown). As putative depletion targets, we consider proteins with high homology to targeted proteins (Table 1), therefore of potential affinity to the corresponding antibody (for example, different complement factors—see S2 Table for the list of excluded proteins). Proteins identified with at least one unique peptide were included in the analysis.

$$\frac{Average\ protein\ area\ based\ on\ top\ 3\ peptides}{Total\ peak\ area\ (of\ non-targets)\ in\ the\ sample\ based\ on\ average\ of\ top\ 3\ peptides\ per\ protein} * 10\hat{}6$$

Immunoglobulin chains were combined into the following proteins, representing the abundant proteins from the group: Ig gamma-1 chain C region (comprising of lambda, gamma and kappa and heavy chains), Ig alpha-1 chain C region (comprising of Ig alpha chains and J chain) and Ig mu chain C region.

Statistical analysis was based on the unequal variance 2-tailed Student's t-test. Proteins with p-value $\leq$0.05 and ratio $\geq$1.5 or $\leq$0.66 were considered as statistically significant. Additionally, in the case of relative protein abundance, obtained p-values were adjusted by applying Benjamini-Hochberg correction for multiple testing.

Results

SDS-PAGE analysis

Four commercially available depletion kits were employed to estimate their efficiency and reproducibility in combination with LC-MS/MS analysis of urinary proteins. Five technical replicates were performed in each case, using urine from normal or CKD patients. In addition, 5 technical replicates of each of the urine from CKD and normal patients (unfractionated – starting material) were analyzed to assess effectiveness of protein depletion. Since the study aims at the evaluation of depletion strategies in biomarker discovery using samples from large clinical cohorts, where typically low-urine volumes are available per researcher, the analysis was performed using a starting volume of 500 μL (without targeting specific starting protein amounts, regularly not feasible in such studies).

Fractionation was performed according to the manufacturer's instructions with minor adaptations, as described in the Materials and Methods section. Bradford assay was performed to estimate the total protein content in urine samples after depletion. Protein amounts at different steps of the analysis, when determined, are presented in Fig 1. The total protein content prior to depletion was estimated at 29 μg (normal) and 437 μg (CKD). In the case of normal sample, the protein content after depletion was below the limit of detection, regardless of the method applied. For the CKD sample, after applying ProteoPrep and SpinTrap kits, the protein content was estimated at 48 μg and 65 μg respectively. The highest protein amount remaining in the sample after depletion was observed for ion-exchange-based ProteoSpin kit, (estimated at 135 μg). For Seppro IgY14, the respective protein content was below the limit of detection. As shown, protein measurements in the depleted fraction vary among different methods, as expected in part based on their specificity.

Depleted urine fractions were then subjected to SDS-PAGE analysis to investigate efficiency and reproducibility of each depletion strategy. Representative gel fractions per method are presented in Fig 2 and all of the analyzed SDS-PAGE gels are shown in S1–S5 Figs. Gel patterns of the depleted fractions indicate reproducibility in all cases (evidenced in S1–S5 Figs), as estimated by their high similarity among technical replicates. As shown based on this gel image analysis, the immuno-based methods appear to have a higher depletion efficiency compared to the ion-exchange strategy, in overall agreement with the measured protein concentration.

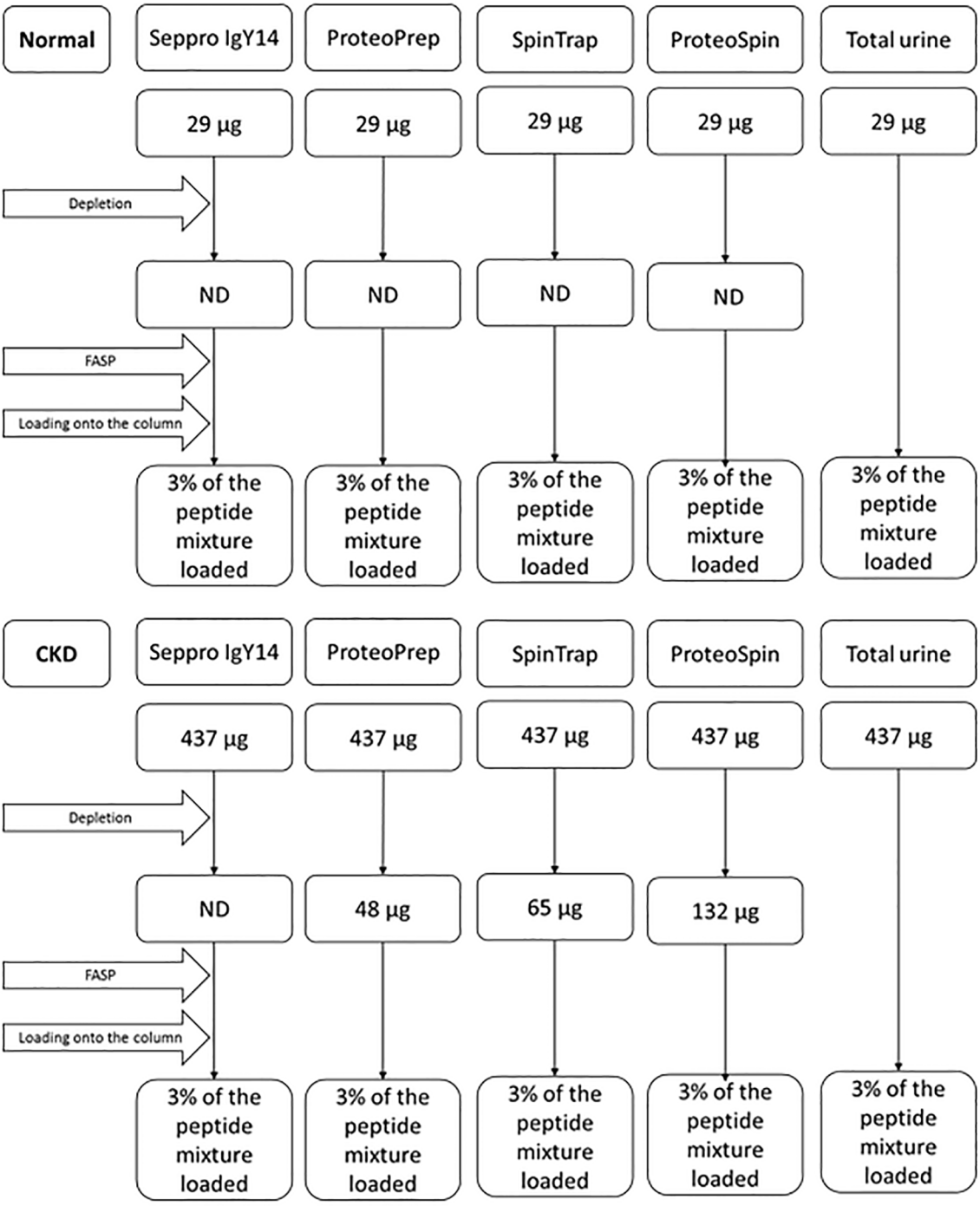

Fig 1. Protein amounts at different steps of the analysis as estimated by Bradford measurements. ND: not determined due to measurements being below the limit of detection (i.e. concentration < 0.2 µg/µL).

doi:10.1371/journal.pone.0133773.g001

Urine peptides and proteins identified by LC-MS/MS

Urine samples prior to or after depletion were processed according to the FASP protocol and analyzed by LC-MS/MS. The numbers of identified peptides per run for each of the five technical replicates per method were compared (Fig 3). For urine of healthy controls, the highest

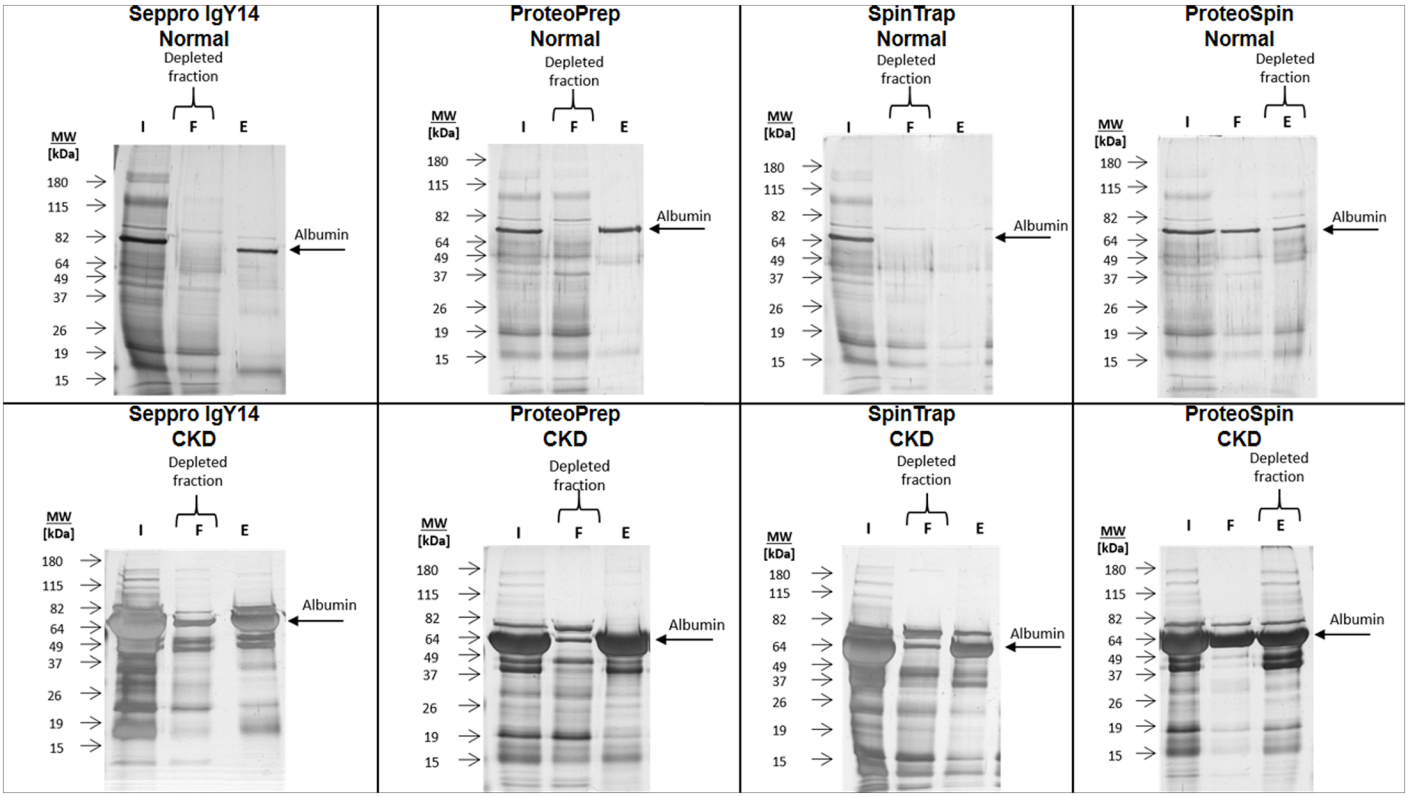

Fig 2. Representative SDS-PAGE results for fractionated and non-fractionated samples (normal and CKD). The figure represents initial urine, flow-through and elution for each of the depletion kits applied. The fractions representing depleted sample and albumin as a common protein depleted by all the kits are marked. I—Initial urine (non-fractionated sample); F—Flow-through fraction; E—Elution. The same protein amounts were loaded onto the gels for initial sample (lane 2 in all cases). Any observed differences in staining intensities are attributed to differences in the silver staining procedure.

doi:10.1371/journal.pone.0133773.g002

number of peptides was identified from the initial (unfractionated) sample (approx. 2,400 peptides) and in the depleted fraction processed by ProteoPrep kit (approx. 2,150 peptides), followed by ProteoSpin, Seppro IgY14 and SpinTrap kits (approx. 1,500 peptides). The most significant differences in the number of identifications, were found between initial urine and

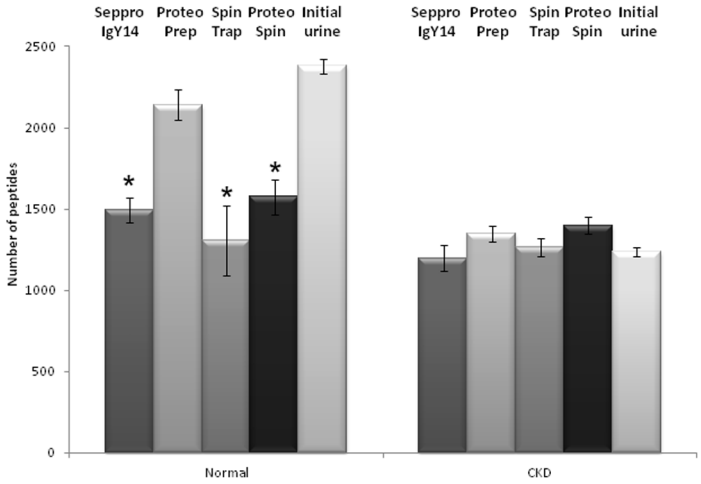

Fig 3. Average number of peptides identified per method.

doi:10.1371/journal.pone.0133773.g003

Table 2. Comparison of the number of peptide identifications, PSMs, search inputs and TICs for normal and CKD sample.

		Normal		
Analysis method	Average number of identified peptides	Average number of PSMs	Average number of Search inputs	Average total ion current [sum of the peak areas]
Seppro IgY14	1495	4978	15813	7.98E+10
ProteoPrep	2142	6263	18092	2.55E+11
SpinTrap	1306	4363	15685	9.07E+10
ProteoSpin	1575	5184	15725	6.73E+10
Total urine	2380	10650	21576	3.86E+11
		CKD		
Seppro IgY14	1197	5646	15905	5.06E+10
ProteoPrep	1350	6980	16628	9.02E+11
SpinTrap	1264	6667	16425	8.26E+10
ProteoSpin	1399	8772	19192	2.00E+11
Total urine	1234	9055	22455	4.34E+11

doi:10.1371/journal.pone.0133773.t002

Seppro IgY14, SpinTrap and ProteoSpin kits (p-value $\leq$ 0.0002). In the case of urine from CKD patients, no significant difference in the number of detected peptides could be observed when comparing the output of the different methods (approx. 1250 peptides in the unfractionated and all depleted fractions).

To rule out that differences in the number of identifications is related to undersampling and/or MS data quality, we investigated the number of obtained peptides, number of PSMs, search inputs (MS/MS scans), and total ion currents (TICs) obtained in each case. As demonstrated in Table 2, the average numbers of PSMs, search inputs and TICs were comparable among CKD and normal samples per depletion strategy. Nevertheless, in the case of CKD, the number of peptide identifications is lower compared to the respective number from normal. This suggests that for CKD, a larger fraction of the MS/MS scans is on the same, highly-abundant peptides.

Comparable numbers of proteins identified in at least three out of five replicates per technique were detected in all cases (approx. 390 in normal and 160 in CKD samples). Overall, more proteins were detectable in the normal urine than in CKD sample (p-value = 0.0002). This observation applies for both total urine and fractionated samples (Table 3). All techniques were found to be reproducible in terms of received protein identifications, as shown in Table 3. In all cases, at least 80% of identified proteins were detected in all 5 replicates.

Table 3. Total number (sum) of identified proteins per depletion strategy for normal and CKD sample (in at least 3, 4 and 5 technical replicates). For both depleted and non-depleted sample the number of identifications is higher in normal than in CKD urine.

		Normal			
Name of the kit	Seppro IgY14	ProteoPrep	SpinTrap	ProteoSpin	Total urine
Proteins identified in 5 replicates	287	387	265	276	362
Proteins identified in 4 replicates	321	420	299	315	397
Proteins identified in 3 replicates	354	466	352	361	431
		CKD			
Name of the kit	Seppro IgY14	ProtoPrep	SpinTrap	ProteoSpin	Total urine
Proteins identified in 5 replicates	113	151	159	116	132
Proteins identified in 4 replicates	124	164	172	126	146
Proteins identified in 3 replicates	137	172	185	139	159

doi:10.1371/journal.pone.0133773.t003

Among the detected proteins, 33% and 36%, which correspond to 205 proteins (normal) or 90 proteins (CKD), are identified by all methods (S6 Fig). These include many highly-abundant proteins such as albumin, vitamin D-binding protein, clusterin, zinc-alpha-2-glycoprotein, uromodulin and beta-2-microglobulin (S2 Table). This "core proteome" corresponds to 53% (+/-7%; normal) and 58% (+/-8%; CKD) of total identifications received per method. In fact, these common proteins correspond to approx. 95% of the total protein peak area in all analyzed samples. The percentage of identified proteins that are unique per analysis method is low, in the range of 10–15% (S2 Table).

To confirm efficiency of analysis, the applied LC-MS/MS protocol was compared to various alternative experimental conditions including: Top 20 versus Top 10 or Top 7 MS/MS analysis; injection of 1 versus 4 μg of protein. In all cases no substantial difference to the presented data could be observed. Importantly, the applied protocol provided average numbers of received MS/MS scans similar to numbers reported in published high resolution datasets [37, 38].

Changes in protein sequence coverage after protein depletion

Peptide sequences per protein identified from the five technical replicates were combined and used for coverage calculations (S2 Table). The coverage from depleted samples was compared with the coverage from initial samples ($\log_2$ ratio depleted/initial urine) (S7–S10 Figs). For all samples from healthy controls, the depletion reduced sequence coverage of protein targets compared to the undepleted urine (from 5% reduction for IgG, up to 90% for serotransferrin in Seppro IgY14 kit). Similarly, in the case of CKD samples, sequence coverage slightly decreased for all depletion targets after application of the albumin and IgG depletion kits (ProteoPrep and SpinTrap) (S8 and S9 Figs). Decrease in the sequence coverage of three target proteins was not observed after fractionation through Seppro IgY14 (S7 Fig): albumin, alpha-1-acid glycoprotein 1 and immunoglobulin alpha. Similarly, sequence coverage did not decrease for alpha-1-antitrypsin after applying ProteoSpin kit (S10 Figs). Among the non-target proteins, no clear trend or impact on sequence coverage could be observed following application of depletion strategies (S7–S10 Figs).

To further investigate this issue, the number of PSMs in relation to sequence coverage was studied. A positive correlation between protein sequence coverage and PSMs could be observed in all cases: if the sequence coverage for a given protein was higher in the depleted sample compared to the unfractionated urine, so was the number of respective PSMs. Similarly, decrease in protein sequence coverage was associated with lower number of PSMs (data not shown). This correlation was in the range of 60%-70% for normal and 70%-80% for CKD samples.

Changes in relative abundance after protein depletion

To estimate the variability in protein abundance between technical replicates, the coefficient of variation for the 50 most abundant proteins from each sample and for the whole protein dataset was calculated (Fig 4). The list of 50 most abundant proteins per method tested is summarized in S3 Table. In the normal urine sample, higher variability was observed for Seppro IgY14, SpinTrap and ProteoSpin (CVs in the range of 26% for 50 most abundant and 40% for whole dataset). ProteoPrep and initial urine demonstrated variabilities in the range of 14% for the 50 most abundant, and 30% for the whole dataset. In the case of CKD samples, all of the analysis strategies demonstrated similar CVs (approx. 10% for 50 most abundant and 28% for the whole dataset), with the exception of Seppro IgY14, which showed a higher CV (27% for the 50 most abundant and 40% for the whole dataset). In all cases the variability increases (by approxiamately 16% for the 50 most abundant proteins) when low-abundance proteins are included in the CV calculations.

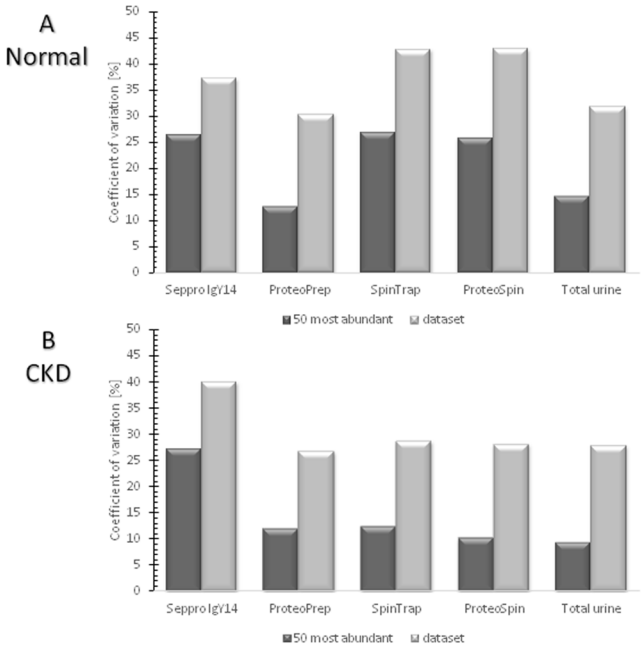

Fig 4. Coefficient of variation for 50 most abundant proteins and whole dataset for A) Normal, B) CKD urine. Normal samples appear having higher variability compared to the CKD samples, nevertheless this difference is not significant. Additionally and as expected, the variability increases when low-abundance proteins are included in the CV calculations.

doi:10.1371/journal.pone.0133773.g004

To evaluate the effect of depletion on relative abundance of proteins, a comparison of relative abundance of individual proteins between a depletion method and the undepleted urine was conducted. The enrichment or depletion of proteins was calculated based on the $\log_2$ ratio of signal intensity in the depleted against initial urine (S11–S14 Figs). Additionally, in Fig 5 the relative abundance of 20 most abundant proteins from undepleted urine (for normal and CKD) was compared to their abundance from corresponding depleted fractions. In the case of depletion targets, the application of immuno-based methods resulted in the reduction of their relative abundance. This observation is valid for urine from both normal and CKD patients. However, for the ion-exchange method (S14 Fig), the depletion was not efficient for serotransferrin in normal urine and for alpha-1-antitrypsin and albumin for CKD. When non-target proteins were compared, no clear trend in the abundance (increase or decrease) was observed. Collectively, similarly to protein sequence coverage, protein depletion had a variable impact on protein abundance, suggesting no added value of these strategies for the analysis of urine samples.

The depletion efficiency of the tested kits was also further estimated as follows: the relative abundance of albumin, as a target for all depletion kits, was compared before and after application of the fractionation strategies. As shown in Fig 5, significant depletion of Albumin was observed for normal samples: (approx. 98% decrease for all three immuno-based methods and 45% decrease for ion-exchange). For the urine from CKD patients, the most efficient depletion was observed for the albumin and IgG depletion kits: SpinTrap ProteoPrep and (95% and 91% decrease respectively), followed by the Seppro IgY14 (63% decrease). The depletion was inefficient in case of using ion-exchange ProteoSpin kit. Collectively, immuno-based methods outperformed the ion-exchange-based strategy in depleting albumin. Additionally, all three immuno-depletion kits depleted albumin with similar efficiency in the case of normal samples, whereas albumin and IgG depletion kits (ProteoPrep and SpinTrap) demonstrated higher

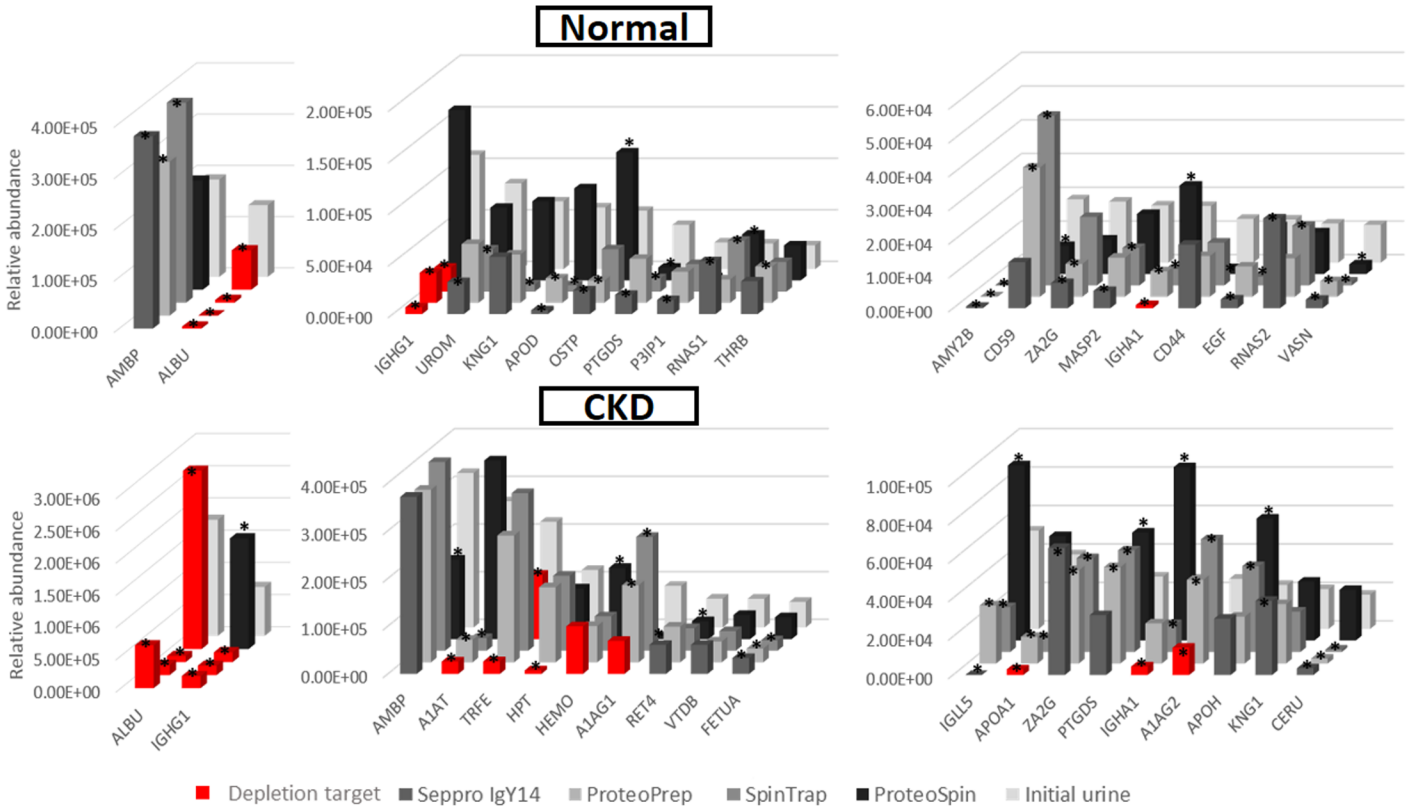

Fig 5. Relative abundance of 20 most abundant proteins derived from undepleted urine and comparison of their abundance with corresponding depleted fractions for urine from healthy controls and CKD patients. Efficient depletion of target proteins is observable for all methods, with the exception of albumin for ProteoSpin in CKD sample. * Denotes significant changes compared to initial urine. ABMP: protein AMBP, ALBU: albumin, IGHG1: Ig gamma-1 chain region, UROM: uromodulin, KNG1: kininogen 1, APOD: apolipoprotein D, OSTP: osteopontin, PTGDS: prostaglandin-H2 D-isomerase, P3IP1: phosphoinositide-3-kinase-interacting protein 1, RNAS1: ribonuclease pancreatic, THRB: prothrombin, AMY2B: alpha-amylase 2B, CD59: CD59 glycoprotein, ZA2G: zinc-alpha-2-glycoprotein, MASP2: mannan-binding lectin serine protease 2, IGHA1: Ig alpha-1 chain C region, CD44: CD44 antigen, EGF: pro-epidermal growth factor, RNAS2: non-secretory ribonuclease, VASN: vasorin, A1AT: alpha-1-antitrypsin, TRFE: serotransferrin, HPT: haptoglobin, HEMO: hemopexin, A1AG1: alpha-1-acid glycoprotein 1, RET4: retinol-binding protein 4, VTDB: vitamin D-binding protein, FETUA: alpha-2-HS-glycoprotein, IGLL5: immunoglobulin lambda-like polypeptide 5, APOA1: apolipoprotein A-I, A1AG2: alpha-1-acid glycoprotein 2, APOH: beta-2-glycoprotein 1, CERU: ceruloplasmin.

doi:10.1371/journal.pone.0133773.g005

depletion effectiveness compared to Seppro IgY14 for CKD. These results are in agreement with the SDS-PAGE analysis (Fig 2), where the highest albumin band intensity reduction was observed for ProteoPrep and SpinTrap, followed by Seppro IgY14 (see SDS-PAGE Analysis section). Of note, the relative abundance of Albumin based on MS data is noticeably higher in the initial CKD sample (approx. 65% of the total peak area) compared to normal (approx. 25% of the total peak area).

Discussion

The main goal of the study was to evaluate the applicability of depletion of abundant proteins in urine samples from CKD patients and controls, at starting volumes regularly available from large clinical cohorts, using commercially available kits, originally designed for plasma. Based on the gel profiles from SDS-PAGE and the number of identified peptides from LC-MS/MS, each depletion strategy is reproducible, and in the case of normal samples, albumin as a target protein is efficiently depleted. For CKD samples, immunodepletion kits efficiently depleted

albumin and the highest efficiency was observed for albumin and IgG depletion kits (ProteoPrep and SpinTrap) followed by Seppro IgY14 (Fig 2 and Fig 5).

The reduced efficiency of Seppro IgY14 may be attributed to potential column overloading-even though this was not expected to be the case based on the manufacturer's instructions: Seppro IgY14 is designed to work with plasma, where the concentration of highly-abundant proteins is substantial. Additionally, the loaded protein amount in this study (437 μg) was not even half of the column binding capacity (1 mg max. column binding capacity). The reason(s) of the lower efficiency of Seppro IgY14 in depleting albumin in CKD urine is still unknown. The ion-exchange-based ProteoSpin kit was found to be the least efficient in eliminating target proteins from both normal and CKD urine. This was expected due to the highly-specific nature of immuno-based mechanism employed in the other kits [15].

Regardless whether a depletion method was applied or not, the number of protein identifications from LC-MS/MS analysis were comparable. In all cases, in the urine from CKD patients fewer proteins were identified in comparison to urine from healthy controls, even though the number of PSMs, MS/MS scans and TICs were similar per method. This may indicate that, even upon depletion, the potential masking effect from highly abundant proteins still exists. After depletion of the target highly-abundant proteins, other non-targeted high and medium-abundance molecules (e.g. protein AMBP, vitamin D-binding proteins, zinc-alpha-2-glycoprotein, uromodulin) likely maintain the masking effect. Alternatively, a large number of proteins may be below the limit of detection (estimated at low femtomole range for the applied mass spectrometer) and therefore, any positive impact of depletion on proteome coverage cannot be observed. Collectively, comparable numbers of received identifications between different strategies, as well as the presence of unique proteins in both fractionated and initial urine indicate no benefit of depletion for biomarker identification purposes.

Our results are not in agreement with Kushnir et al. [30] findings, where the employment of a multiple affinity removal (MARS) column allowed increasing the number of identifications in urine from 60 to 142 in CKD patients. Still, in our presented study the number of protein identifications is higher in comparison, possibly a result of a less sensitive instrument used by the authors (Q-TOF equipped with a ChipCube). The immuno-based depletion strategies were also evaluated in 2D gel proteomics experiments [24, 27, 39, 40]. In these cases the number of unique identifications did not change significantly following depletion.

In order to evaluate the validity of the obtained protein identifications from urine from healthy controls, 100 most abundant (as the most reliable) proteins from each analysis method (i.e. undepleted and fractionated samples), were compared with the identifications from three manuscripts reporting on the analysis of urine proteome from healthy individuals [41–43]. In each case, approx. 90 out of the 100 most abundant proteins identified in the present study were also reported in these manuscripts. When expanding the comparison from the 100 most abundant to the whole dataset an overlap of approx. 60%, for the normal samples was observed, similar to the overlap of protein identifications between the three different studies. These similarities between different datasets representing normal urine support the validity of our data. To estimate the validity of obtained identifications from CKD samples, proteins from all CKD datasets were compared with molecules associated with renal diseases reported in the literature [44–46]. Due to the too small sample size tested to evaluate differential expression of these molecules, our focus was set only on their presence. Several of these disease-associated proteins were identified in all datasets (i.e. albumin, neutrophil gelatinase-associated lipocalin, cystatin C, osteopontin, clusterin, beta-2-microglobulin). A few were unique for applied strategies: metalloproteinase inhibitor 1 was present in three kits (Seppro IgY14, SpinTrap and ProteoSpin), fatty acid-binding protein was unique for unfractionated sample and connective tissue growth factor for SpinTrap kit.

Based on the available literature data and in line to our observations, a number of non-targeted proteins are also depleted to some degree [23–25], negatively affecting the analysis. This effect may be related to the fact that targeted proteins may form stable complexes with non-targeted proteins resulting in their co-depletion. This co-depletion mechanism was observed in a number of studies (i.e. [23–25]). For example, Granger et al. [23] demonstrated that depletion of albumin removed also low-abundance proteins including cytokines from plasma samples. Similarly, Stempfer et al. [25], spiked 6 recombinant cytokines in serum samples and showed that application of depletion methods reduced the cytokine levels.

The application of depletion strategies did not improve the proteome or sequence coverage. Given that the overall data quality and quantity (as reflected by the number of MS/MS scans—Table 2) were not significantly affected following fractionation, the fact that no clear increase in proteome and sequence coverage could be observed may be attributed to the following factors: proteome complexity rendering effects of depletion per protein are unpredictable, lack of sufficient depletion to generate an observable impact on coverage as well as peptides (even if enriched) still remaining below the limit of detection (i.e. undersampling at an individual protein level).

Comparison of changes in protein abundance for overlapping identifications prior to and after depletion was also performed by Tu et al. [26] for plasma samples using MARS columns. In contrast to the present study, where no clear advantage of protein depletion was observed, the authors found that most of the non-targeted proteins were enriched after depletion. This discrepancy may be related to: i) depletion was evaluated in plasma samples, not urine, and ii) significantly higher starting protein content was used.

Target proteins were less efficiently depleted in the urine from CKD patients compared to normal, regardless of the depletion strategy applied, even though the protein content loaded onto the depletion column was always (according to the manufacturers protocols) below their loading capacity. However, it may be that the actual loading capacity is lower than claimed.

In conclusion, the depletion of abundant proteins does not present an added value for the study of the urine proteome, at least when starting with small urine volumes (less than 1 mL), regularly available in large clinical studies. No significant improvement in the number of identifications, protein sequence coverage or relative abundance in comparison to the undepleted samples were detected using different methods in the current study. Moreover, the depletion introduced additional variability. Depletion of targeted proteins was substantially more efficient in normal than for CKD samples, suggesting that additional disease-related factors may impair the depletion efficiency. Therefore, for the urinary proteomics studies especially in the context of CKD, analysis of total rather than depleted urine appears preferable.

Supporting Information

S1 Table. Peptide lists for all analysis methods.
(XLSX)

S2 Table. Lists of common and unique identifications for depleted samples and initial urine for all strategies.
(XLSX)

S3 Table. 50 most abundant proteins for each depletion strategy and unfractionated sample for normal and CKD urine. X denotes that the protein was found as one of the 50 most abundant in the respective analysis method.
(XLSX)

S1 Fig. SDS-PAGE gel profiles for Seppro IgY14 depletion kit for normal samples: Depleted fractions and albumin as a target protein are marked. M—molecular size marker. I—initial urine. F—Flow-through fraction. W—Wash. E—Elution. 1–4 –consecutive numbers of flow-through/wash/elution within one replicate.
(TIF)

S2 Fig. SDS-PAGE gel profiles for Seppro IgY14 depletion kit for CKD samples: Depleted fractions and albumin as a target protein are marked. M—molecular size marker. I—initial urine. F—Flow-through fraction. W—Wash. E—Elution. 1–4 –consecutive numbers of flow-through/wash/elution within one replicate.
(TIF)

S3 Fig. SDS-PAGE gel profiles for ProtePrep depletion kit. Depleted fractions and albumin as a target protein are marked. M—molecular size marker. I—initial urine. F—Flow-through fraction. E—Elution. I-V—number of technical replicate.
(TIF)

S4 Fig. SDS-PAGE gel profiles for SpinTrap depletion kit. Depleted fractions and albumin as a target protein are marked. M—molecular size marker. I—initial urine. F—Flow-through fraction. E—Elution. I-V—number of technical replicate.
(TIF)

S5 Fig. SDS-PAGE gel profiles for ProteoSpin depletion kit. Depleted fractions and albumin as a target protein are marked. M—molecular size marker. I—initial urine. F—Flow-through fraction. E—Elution. I-V—number of technical replicate.
(TIF)

S6 Fig. Venn Diagram [47]: unique identifications for urine from A) normal B) CKD patients. In total 612 and 251 unique proteins, in at least three out of five replicates, were identified in normal and CKD samples respectively. Approximately 33% of the identifications are shared between non-depleted and depleted urine in normal or CKD sample.
(TIF)

S7 Fig. Changes in protein sequence coverage for overlapping identifications between Seppro IgY14 depleted sample and initial urine. X axis represents the protein sequence coverage of the initial urine. The changes after applying the depletion strategy are presented on Y-axis (with $\log_2$ scale) as a ratio of depleted versus non-depleted sample. Proteins, with increased sequence coverage are presented above the ratio of 0 on the Y-scale and with decreased below the ratio of 0. Proteins with a ratio of 0 show the same coverage in the initial and depleted sample. Sequence coverage for immunoglobulins is presented as an average coverage for all proteins combined in the group. Protein targets for depletion kit are marked as red dots (see Table 1). Protein targets for which the protein sequence coverage increased after depletion are marked by an arrow.
(TIF)

S8 Fig. Changes in protein sequence coverage for overlapping identifications between ProteoPrep depleted sample and initial urine. X axis represents the protein sequence coverage of the initial urine. The changes after applying the depletion strategy are presented on Y-axis (with $\log_2$ scale) as a ratio of depleted versus non-depleted sample. Proteins, with increased sequence coverage are presented above the ratio of 0 on the Y-scale and with decreased below the ratio of 0. Proteins with a ratio of 0 show the same coverage in the initial and depleted sample. Sequence coverage for immunoglobulins is presented as an average

coverage for all proteins combined in the group. Protein targets for depletion kit are marked as red dots (see Table 1).
(TIF)

S9 Fig. Changes in protein sequence coverage for overlapping identifications between SpinTrap depleted sample and initial urine. X axis represents the protein sequence coverage of the initial urine. The changes after applying the depletion strategy are presented on Y-axis (with $\log_2$ scale) as a ratio of depleted versus non-depleted sample. Proteins, with increased sequence coverage are presented above the ratio of 0 on the Y-scale and with decreased below the ratio of 0. Proteins with a ratio of 0 show the same coverage in the initial and depleted sample. Sequence coverage for immunoglobulins is presented as an average coverage for all proteins combined in the group. Protein targets for depletion kit are marked as red dots (see Table 1).
(TIF)

S10 Fig. Changes in protein sequence coverage for overlapping identifications between ProteoSpin depleted sample and initial urine. X axis represents the protein sequence coverage of the initial urine. The changes after applying the depletion strategy are presented on Y-axis (with $\log_2$ scale) as a ratio of depleted versus non-depleted sample. Proteins, with increased sequence coverage are presented above the ratio of 0 on the Y-scale and with decreased below the ratio of 0. Proteins with a ratio of 0 show the same coverage in the initial and depleted sample. Sequence coverage for immunoglobulins is presented as an average coverage for all proteins combined in the group. Protein targets for depletion kit are marked as red dots (see Table 1). Protein targets for which the protein sequence coverage increased after depletion are marked by an arrow.
(TIF)

S11 Fig. Changes in protein abundance for overlapping identifications between Seppro IgY14 depleted sample and initial urine. The scatterplots present the protein relative abundance changes after protein depletion in comparison to the initial sample. X axis represents the normalized protein abundance for initial urine in logarithmic scale ($\log_2$). Proteins on the Y axis ($\log_2$ scale) above a ratio of 0 are enriched in comparison to initial urine, while those below the ratio of 0 are depleted. Proteins with a ratio 0 show the same relative abundance in the initial and depleted sample. Protein abundance for immunoglobulins is presented as a sum of the abundance for all combined proteins in the group. Protein targets for depletion kit are marked as red dots (see Table 1).
(TIF)

S12 Fig. Changes in protein abundance for overlapping identifications between ProteoPrep depleted sample and initial urine. The scatterplots present the protein relative abundance changes after protein depletion in comparison to the initial sample. X axis represents the normalized protein abundance for initial urine in logarithmic scale ($\log_2$). Proteins on the Y axis ($\log_2$ scale) above a ratio of 0 are enriched in comparison to initial urine, while those below the ratio of 0 are depleted. Proteins with a ratio 0 show the same relative abundance in the initial and depleted sample. Protein abundance for immunoglobulins is presented as a sum of the abundance for all combined proteins in the group. Protein targets for depletion kit are marked as red dots (see Table 1).
(TIF)

S13 Fig. Changes in protein abundance for overlapping identifications between SpinTrap depleted sample and initial urine. The scatterplots present the protein relative abundance

changes after protein depletion in comparison to the initial sample. X axis represents the normalized protein abundance for initial urine in logarithmic scale (log_2). Proteins on the Y axis (log_2 scale) above a ratio of 0 are enriched in comparison to initial urine, while those below the ratio of 0 are depleted. Proteins with a ratio 0 show the same relative abundance in the initial and depleted sample. Protein abundance for immunoglobulins is presented as a sum of the abundance for all combined proteins in the group. Protein targets for depletion kit are marked as red dots (see Table 1).
(TIF)

S14 Fig. Changes in protein abundance for overlapping identifications between ProteoSpin depleted sample and initial urine. The scatterplots present the protein relative abundance changes after protein depletion in comparison to the initial sample. X axis represents the normalized protein abundance for initial urine in logarithmic scale (log_2). Proteins on the Y axis (log_2 scale) above a ratio of 0 are enriched in comparison to initial urine, while those below the ratio of 0 are depleted. Proteins with a ratio 0 show the same relative abundance in the initial and depleted sample. Protein abundance for immunoglobulins is presented as a sum of the abundance for all combined proteins in the group. Protein targets for depletion kit are marked as red dots (see Table 1). Protein targets for which the relative abundance increased after depletion are marked by an arrow.
(TIF)

Author Contributions

Conceived and designed the experiments: SF KV JZ WM HM AV. Performed the experiments: SF KV WM. Analyzed the data: SF AL. Contributed reagents/materials/analysis tools: KV WM AV. Wrote the paper: SF JZ AL GS HM AV JJ.

References

1. Yates JR, Ruse CI, Nakorchevsky A. Proteomics by mass spectrometry: approaches, advances, and applications. Annual review of biomedical engineering. 2009; 11:49–79. doi: 10.1146/annurev-bioeng-061008-124934 PMID: 19400705.
2. Law KP, Lim YP. Recent advances in mass spectrometry: data independent analysis and hyper reaction monitoring. Expert review of proteomics. 2013; 10(6):551–66. doi: 10.1586/14789450.2013.858022 PMID: 24206228.
3. Fliser D, Novak J, Thongboonkerd V, Argiles A, Jankowski V, Girolami MA, et al. Advances in urinary proteome analysis and biomarker discovery. Journal of the American Society of Nephrology: JASN. 2007; 18(4):1057–71. doi: 10.1681/ASN.2006090956 PMID: 17329573.
4. Anderson NL, Anderson NG. The human plasma proteome: history, character, and diagnostic prospects. Molecular & cellular proteomics: MCP. 2002; 1(11):845–67. PMID: 12488461.
5. Thomas R, Kanso A, Sedor JR. Chronic kidney disease and its complications. Primary care. 2008; 35 (2):329–44, vii. doi: 10.1016/j.pop.2008.01.008 PMID: 18486718; PubMed Central PMCID: PMC2474786.
6. Filip S, Pontillo C, Peter Schanstra J, Vlahou A, Mischak H, Klein J. Urinary proteomics and molecular determinants of chronic kidney disease: possible link to proteases. Expert review of proteomics. 2014:1–14. doi: 10.1586/14789450.2014.926224 PMID: 24957818.
7. Perkins BA, Ficociello LH, Roshan B, Warram JH, Krolewski AS. In patients with type 1 diabetes and new-onset microalbuminuria the development of advanced chronic kidney disease may not require progression to proteinuria. Kidney international. 2010; 77(1):57–64. doi: 10.1038/ki.2009.399 PMID: 19847154; PubMed Central PMCID: PMC3725722.
8. Rifai N, Gillette MA, Carr SA. Protein biomarker discovery and validation: the long and uncertain path to clinical utility. Nature biotechnology. 2006; 24(8):971–83. doi: 10.1038/nbt1235 PMID: 16900146.
9. Decramer S, Gonzalez de Peredo A, Breuil B, Mischak H, Monsarrat B, Bascands JL, et al. Urine in clinical proteomics. Molecular & cellular proteomics: MCP. 2008; 7(10):1850–62. doi: 10.1074/mcp.R800001-MCP200 PMID: 18667409.

10. Hortin GL, Sviridov D. Diagnostic potential for urinary proteomics. Pharmacogenomics. 2007; 8 (3):237–55. doi: 10.2217/14622416.8.3.237 PMID: 17324112.

11. Doucette AA, Tran JC, Wall MJ, Fitzsimmons S. Intact proteome fractionation strategies compatible with mass spectrometry. Expert review of proteomics. 2011; 8(6):787–800. doi: 10.1586/epr.11.67 PMID: 22087661.

12. Jungbauer A, Hahn R. Ion-exchange chromatography. Methods in enzymology. 2009; 463:349–71. doi: 10.1016/S0076-6879(09)63022-6 PMID: 19892182.

13. Duong-Ly KC, Gabelli SB. Gel filtration chromatography (size exclusion chromatography) of proteins. Methods in enzymology. 2014; 541:105–14. doi: 10.1016/B978-0-12-420119-4.00009-4 PMID: 24674066.

14. Cheung RC, Wong JH, Ng TB. Immobilized metal ion affinity chromatography: a review on its applications. Applied microbiology and biotechnology. 2012; 96(6):1411–20. doi: 10.1007/s00253-012-4507-0 PMID: 23099912.

15. Moser AC, Hage DS. Immunoaffinity chromatography: an introduction to applications and recent developments. Bioanalysis. 2010; 2(4):769–90. doi: 10.4155/bio.10.31 PMID: 20640220; PubMed Central PMCID: PMC2903764.

16. Urh M, Simpson D, Zhao K. Affinity chromatography: general methods. Methods in enzymology. 2009; 463:417–38. doi: 10.1016/S0076-6879(09)63026-3 PMID: 19892186.

17. Filip S, Zoidakis J, Vlahou A, Mischak H. Advances in urinary proteome analysis and applications in systems biology. Bioanalysis. 2014; 6(19):2549–69. doi: 10.4155/bio.14.210 PMID: 25411698.

18. Righetti PG, Candiano G, Citterio A, Boschetti E. Combinatorial Peptide ligand libraries as a "trojan horse" in deep discovery proteomics. Analytical chemistry. 2015; 87(1):293–305. doi: 10.1021/ac502171b PMID: 25084147.

19. Righetti PG, Boschetti E. The ProteoMiner and the FortyNiners: searching for gold nuggets in the proteomic arena. Mass spectrometry reviews. 2008; 27(6):596–608. doi: 10.1002/mas.20178 PMID: 18481254.

20. Boschetti E, Giorgio Righetti P. Hexapeptide combinatorial ligand libraries: the march for the detection of the low-abundance proteome continues. BioTechniques. 2008; 44(5):663–5. doi: 10.2144/000112762 PMID: 18474042.

21. Righetti PG, Boschetti E. Sample treatment methods involving combinatorial Peptide ligand libraries for improved proteomes analyses. Methods in molecular biology. 2015; 1243:55–82. doi: 10.1007/978-1-4939-1872-0_4 PMID: 25384740.

22. Millioni R, Tolin S, Puricelli L, Sbrignadello S, Fadini GP, Tessari P, et al. High abundance proteins depletion vs low abundance proteins enrichment: comparison of methods to reduce the plasma proteome complexity. PloS one. 2011; 6(5):e19603. doi: 10.1371/journal.pone.0019603 PMID: 21573190; PubMed Central PMCID: PMC3087803.

23. Granger J, Siddiqui J, Copeland S, Remick D. Albumin depletion of human plasma also removes low abundance proteins including the cytokines. Proteomics. 2005; 5(18):4713–8. doi: 10.1002/pmic.200401331 PMID: 16281180.

24. Fountoulakis M, Juranville JF, Jiang L, Avila D, Roder D, Jakob P, et al. Depletion of the high-abundance plasma proteins. Amino acids. 2004; 27(3–4):249–59. doi: 10.1007/s00726-004-0141-1 PMID: 15592754.

25. Stempfer R, Kubicek M, Lang IM, Christa N, Gerner C. Quantitative assessment of human serum high-abundance protein depletion. Electrophoresis. 2008; 29(21):4316–23. doi: 10.1002/elps.200800211 PMID: 18956433.

26. Tu C, Rudnick PA, Martinez MY, Cheek KL, Stein SE, Slebos RJ, et al. Depletion of abundant plasma proteins and limitations of plasma proteomics. Journal of proteome research. 2010; 9(10):4982–91. doi: 10.1021/pr100646w PMID: 20677825; PubMed Central PMCID: PMC2948641.

27. Echan LA, Tang HY, Ali-Khan N, Lee K, Speicher DW. Depletion of multiple high-abundance proteins improves protein profiling capacities of human serum and plasma. Proteomics. 2005; 5(13):3292–303. doi: 10.1002/pmic.200401228 PMID: 16052620.

28. Kullolli M, Warren J, Arampatzidou M, Pitteri SJ. Performance evaluation of affinity ligands for depletion of abundant plasma proteins. Journal of chromatography B, Analytical technologies in the biomedical and life sciences. 2013; 939:10–6. doi: 10.1016/j.jchromb.2013.09.008 PMID: 24090752.

29. Magistroni R, Ligabue G, Lupo V, Furci L, Leonelli M, Manganelli L, et al. Proteomic analysis of urine from proteinuric patients shows a proteolitic activity directed against albumin. Nephrology, dialysis, transplantation: official publication of the European Dialysis and Transplant Association—European Renal Association. 2009; 24(5):1672–81. doi: 10.1093/ndt/gfp020 PMID: 19211645.

30. Kushnir MM, Mrozinski P, Rockwood AL, Crockett DK. A depletion strategy for improved detection of human proteins from urine. Journal of biomolecular techniques: JBT. 2009; 20(2):101–8. PMID: 19503621; PubMed Central PMCID: PMC2685607.

31. Afkarian M, Bhasin M, Dillon ST, Guerrero MC, Nelson RG, Knowler WC, et al. Optimizing a proteomics platform for urine biomarker discovery. Molecular & cellular proteomics: MCP. 2010; 9(10):2195–204. doi: 10.1074/mcp.M110.000992 PMID: 20511394; PubMed Central PMCID: PMC2957724.

32. Magagnotti C, Fermo I, Carletti RM, Ferrari M, Bachi A. Comparison of different depletion strategies for improving resolution of the human urine proteome. Clinical chemistry and laboratory medicine: CCLM / FESCC. 2010; 48(4):531–5. doi: 10.1515/CCLM.2010.109 PMID: 20148726.

33. Chen CL, Lin TS, Tsai CH, Wu CC, Chung T, Chien KY, et al. Identification of potential bladder cancer markers in urine by abundant-protein depletion coupled with quantitative proteomics. Journal of proteomics. 2013; 85:28–43. doi: 10.1016/j.jprot.2013.04.024 PMID: 23631828.

34. Chevallet M, Luche S, Rabilloud T. Silver staining of proteins in polyacrylamide gels. Nature protocols. 2006; 1(4):1852–8. doi: 10.1038/nprot.2006.288 PMID: 17487168; PubMed Central PMCID: PMC1971133.

35. Wisniewski JR, Zougman A, Nagaraj N, Mann M. Universal sample preparation method for proteome analysis. Nature methods. 2009; 6(5):359–62. doi: 10.1038/nmeth.1322 PMID: 19377485.

36. Serang O, Noble W. A review of statistical methods for protein identification using tandem mass spectrometry. Statistics and its interface. 2012; 5(1):3–20. PMID: 22833779; PubMed Central PMCID: PMC3402235.

37. Goo YA, Cain K, Jarrett M, Smith L, Voss J, Tolentino E, et al. Urinary proteome analysis of irritable bowel syndrome (IBS) symptom subgroups. Journal of proteome research. 2012; 11(12):5650–62. doi: 10.1021/pr3004437 PMID: 22998556; PubMed Central PMCID: PMC3631108.

38. Goo YA, Tsai YS, Liu AY, Goodlett DR, Yang CC. Urinary proteomics evaluation in interstitial cystitis/painful bladder syndrome: a pilot study. International braz j urol: official journal of the Brazilian Society of Urology. 2010; 36(4):464–78; discussion 78–9, 79. PMID: 20815953.

39. Martin-Lorenzo M, Gonzalez-Calero L, Zubiri I, Diaz-Payno PJ, Sanz-Maroto A, Posada-Ayala M, et al. Urine 2DE proteome analysis in healthy condition and kidney disease. Electrophoresis. 2014; 35 (18):2634–41. doi: 10.1002/elps.201300601 PMID: 24913465.

40. Polaskova V, Kapur A, Khan A, Molloy MP, Baker MS. High-abundance protein depletion: comparison of methods for human plasma biomarker discovery. Electrophoresis. 2010; 31(3):471–82. doi: 10.1002/elps.200900286 PMID: 20119956.

41. Zerefos PG, Aivaliotis M, Baumann M, Vlahou A. Analysis of the urine proteome via a combination of multi-dimensional approaches. Proteomics. 2012; 12(3):391–400. doi: 10.1002/pmic.201100212 PMID: 22140069.

42. Mischak H, Kolch W, Aivaliotis M, Bouyssie D, Court M, Dihazi H, et al. Comprehensive human urine standards for comparability and standardization in clinical proteome analysis. Proteomics Clinical applications. 2010; 4(4):464–78. doi: 10.1002/prca.200900189 PMID: 21137064; PubMed Central PMCID: PMC3064949.

43. Adachi J, Kumar C, Zhang Y, Olsen JV, Mann M. The human urinary proteome contains more than 1500 proteins, including a large proportion of membrane proteins. Genome biology. 2006; 7(9):R80. doi: 10.1186/gb-2006-7-9-R80 PMID: 16948836; PubMed Central PMCID: PMC1794545.

44. Brott DA, Adler SH, Arani R, Lovick SC, Pinches M, Furlong ST. Characterization of renal biomarkers for use in clinical trials: biomarker evaluation in healthy volunteers. Drug design, development and therapy. 2014; 8:227–37. doi: 10.2147/DDDT.S54956 PMID: 24611000; PubMed Central PMCID: PMC3928457.

45. Fassett RG, Venuthurupalli SK, Gobe GC, Coombes JS, Cooper MA, Hoy WE. Biomarkers in chronic kidney disease: a review. Kidney international. 2011; 80(8):806–21. doi: 10.1038/ki.2011.198 PMID: 21697815.

46. Mischak H, Delles C, Vlahou A, Vanholder R. Proteomic biomarkers in kidney disease: issues in development and implementation. Nature reviews Nephrology. 2015; 11(4):221–32. doi: 10.1038/nrneph.2014.247 PMID: 25643662.

47. Available: http://bioinformatics.psb.ugent.be/webtools/Venn/.

RESEARCH ARTICLE

α-1-Antitrypsin detected by MALDI imaging in the study of glomerulonephritis: Its relevance in chronic kidney disease progression

Andrew Smith[1], Vincenzo L'Imperio[2*], Gabriele De Sio[1], Franco Ferrario[2], Carla Scalia[2], Giacomo Dell'Antonio[3], Federico Pieruzzi[4], Claudia Pontillo[5,6], Szymon Filip[6,7], Katerina Markoska[8], Antonio Granata[9], Goce Spasovski[8], Joachim Jankowski[10], Giovambattista Capasso[11], Fabio Pagni[2] and Fulvio Magni[1]*

[1] Unit of Proteomics, Department of Health Sciences, University of Milano-Bicocca, Monza, Italy
[2] Unit of Pathology, Department of Surgery and Translational Medicine, University of Milano-Bicocca, Monza, Italy
[3] Department of Pathology, San Raffaele Hospital, Milan, Italy
[4] Unit of Nephrology, Department of Health Sciences, University of Milano-Bicocca, Milan, Italy
[5] Mosaiques Diagnostics GmbH, Hannover, Germany
[6] Charité – Universitätsmedizin Berlin, Berlin, Germany
[7] Biomedical Research Foundation Academy of Athens, Athens, Greece
[8] Department of Nephrology, Medical Faculty, University of Skopje, Skopje, Macedonia
[9] Department of Nephrology, Ospedale San Giovanni di Dio, Agrigento, Italy
[10] Institute for Molecular Cardiovascular Research, University Hospital RWTH Aachen, Aachen, Germany
[11] Department of Cardio-Thoracic and Respiratory Science, Second University of Naples, Naples, Italy

Received: October 22, 2015
Revised: November 16, 2015
Accepted: January 4, 2016

Idiopathic glomerulonephritis (GN), such as membranous glomerulonephritis, focal segmental glomerulosclerosis (FSGS), and IgA nephropathy (IgAN), represent the most frequent primary glomerular kidney diseases (GKDs) worldwide. Although the renal biopsy currently remains the gold standard for the routine diagnosis of idiopathic GN, the invasiveness and diagnostic difficulty related with this procedure highlight the strong need for new diagnostic and prognostic biomarkers to be translated into less invasive diagnostic tools. MALDI-MS imaging MALDI-MSI was applied to fresh-frozen bioptic renal tissue from patients with a histological diagnosis of FSGS ($n = 6$), IgAN, ($n = 6$) and membranous glomerulonephritis ($n = 7$), and from controls ($n = 4$) in order to detect specific molecular signatures of primary glomerulonephritis. MALDI-MSI was able to generate molecular signatures capable to distinguish between normal kidney and pathological GN, with specific signals (m/z 4025, 4048, and 4963) representing potential indicators of chronic kidney disease development. Moreover, specific disease-related signatures (m/z 4025 and 4048 for FSGS, m/z 4963 and 5072 for IgAN) were detected. Of these signals, m/z 4048 was identified as α-1-antitrypsin and was shown to be localized to the podocytes within sclerotic glomeruli by immunohistochemistry. α-1-Antitrypsin could be one of the markers of podocyte stress that is correlated with the development of FSGS due to both an excessive loss and a hypertrophy of podocytes.

Keywords:
Biomedicine / Biopsy / Glomerulonephritis / MALDI imaging / Mass spectrometry

Correspondence: Dr. Fulvio Magni, Department of Health Sciences, University of Milano-Bicocca, Piazza dell'Ateneo Nuovo, 1, 20126 Milano, Italy
E-mail: fulvio.magni@unimib.it
Fax: +39-02-6448252

Abbreviations: **A1AT**, α-1-antitrypsin; **CKD**, chronic kidney disease; **eGFR**, estimated glomerular filtration rate; **FFPE**, formalin-fixed paraffin-embedded; **FSGS**, focal segmental glomerulosclerosis; **GKD**, glomerular kidney disease; **GN**, Idiopathic glomerulonephritis; **IgAN**, IgA nephropathy; **MGN**, membranous glomerulonephritis; **SA**, sinapinic acid

*These authors contributed equally to the work.

Colour Online: See the article online to view Figs. 1–3 in colour.

Significance of the study

The body of work enclosed in this manuscript presents MALDI imaging as tool useful for detecting molecular signatures of glomerulonephritis and highlights the added value of correlating in situ proteomic information with urinary proteomics when attempting to identify translatable disease markers. Such molecular signatures could potentially assist in the routine diagnosis of idiopathic glomerulonephritis, where there is a need for less-invasive markers due to the potential complications and diagnostic difficulty associated with the renal biopsy. Specifically, the study employs MS imaging and immunohistochemistry to identify and validate one particular protein, α-1-antitrypsin (A1AT), which was found to be localized in the podocytes of sclerotic glomeruli. This finding suggests that A1AT may be implicated in the development of sclerotic lesions and could represent a marker of podocyte stress, an early sign of glomerulonephritis progression. Several fragments of this protein were also detected in urine and were shown to be overexpressed in the urine of patients who progressed to the latter stages of chronic kidney disease. Therefore, A1AT may represent a potential noninvasive proteomic indicator of the progression of glomerulonephritis.

1 Introduction

Glomerular kidney disease (GKD) represents the third leading cause of end-stage renal disease in Western countries [1]. Clinicians classify GKD in primary and secondary forms based on etiopathogenetic criteria. The former includes idiopathic glomerulonephritis (GN), such as membranous glomerulonephritis (MGN), focal segmental glomerulosclerosis (FSGS), and IgA nephropathy (IgAN), which represent the most frequent primary GKDs worldwide [2, 3]. Currently, the renal biopsy remains the gold standard for routine diagnosis [4]. However, the availability of pathological renal tissue also provides a great opportunity for the research of new diagnostic and prognostic markers that are potentially transferable into less invasive diagnostic tools if they are also detectable in biological fluids such as urine or serum. For this purpose, proteomic approaches are currently very promising and, among them, MALDI-MS imaging (MALDI-MSI) represents a potential technology that can be employed for biomarker discovery, providing the capability to match traditional morphological data related with pathology to proteomic information. Recent feasibility studies showed the possible application of MALDI-MSI in this field, showing the existence of alterations in the tissue protein profiles of MGN and minimal change disease patients [5]. Interestingly, these modifications were observed not only in tissue areas with evident pathological alterations, but also in regions with morphologically normal appearance, thus highlighting the potentiality of MALDI-MSI in nephropathology. In this complex background, we analyzed fresh-frozen tissue from heterogeneous forms of primary GN (FSGS, IgA, and MGN) by MALDI-MSI in order to investigate the potential application of this technique in GNs more deeply and explore the identification of possible new indicators of chronic kidney disease (CKD) progression.

2 Materials and methods

2.1 Materials

Conductive indium tin oxide glass slides, Protein Calibration Standard I and Peptide Calibration Standard I were purchased from Bruker Daltonik GmbH (Bremen, Germany). Sinapinic acid (SA), α-cyano-4-hydroxycinnamic acid (CHCA), HPLC grade acetonitrile, ethanol, and TFA were purchased from Sigma-Aldrich Chemie (Buchs, Switzerland). Tissue-Tek® O.C.T. Compound was obtained from Sakura® Finetek (Alphen aan den Rijn, Netherlands). Alpha-1 antitrypsin (A1AT) polyclonal rabbit Ab was purchased from Dako (Glostrup, Denmark).

2.2 Tissue samples

The study included only primary GNs classified as idiopathic according to the strong clinical criteria presented in (Table 1). Fresh-frozen biopsies taken from patients, who underwent renal biopsy with a histological diagnosis of FSGS ($n = 6$), IgAN ($n = 6$), and MGN ($n = 7$), were collected. Normal cortical biopsies (controls, $n = 4$) corresponded to regions of kidney obtained from radical nephrectomy during tumour treatment. Control patients had no history of functional renal disease. The study was approved by the local Ethical Boards. Renal specimens were embedded in Tissue-Tek optimal cutting temperature within 30 min of biopsy execution or surgical procedure.

2.3 Sample preparation

For each specimen, two 4-μm-thick sections were cut and thaw mounted on the same conductive indium tin oxide glass slide (Bruker Daltonik GmbH) and stabilised for 30 min in a conventional dry oven at 85°C (Tecnovetro s.r.l., Monza,

Table 1. Clinical criteria used to determine the primitivity of MGN, FSGS and IgAN patients

	Criteria
MGN	- Antinuclear antibodies (ANA) below a titer of 1:80 - Negativity for anti-double stranded DNA antibodies - Absence of histological signs of lupus membranous nephritis (type V lupus nephritis) - Negative HBV and HCV serology - Negativity for malignancy
FSGS	- Serological negativity to HIV1, SV40, CMV, EBV, parvovirus B19 - No history of systemic hypertension - No renal dysgenesia/abnormalities - No history of drug abuse
IgAN	- Clinical presentation inconsistent for Henoch–Schoenlein purpura - Negative serology for HCV infection

Italy). The slides were then stored at −80°C until the day of analysis. Glass slides were thawed by desiccation for 30 min and then washed in a graded series of ethanol (70, 90, and 95%). Following the washes, they were again dried for 10 min via desiccation. SA was deposited on the slide through a sublimation apparatus (plate diameter 10 cm, S.B.L. Apparecchi Scientifici, Vimodrone, Italy) with 500 mg of SA at 145°C and 90 mTorr for 30 min [5]. Sublimation was followed by automated spraying of the SA (10 mg/mL in 60%/0.2% v/v acetonitrile/TFA) using the ImagePrep (Bruker Daltonik GmbH) to attain the desired matrix thickness. For the identification process, α-cyano-4-hydroxycinnamic acid (7 mg/mL in 50%/0.1% v/v acetonitrile/TFA) was deposited onto consecutive sections sectioned from the previously used renal specimens using the ImagePrep automated sprayer. The matrix was removed from the tissue by washing with a 50%/0.1% v/v acetonitrile/TFA solution. The resulting solution was concentrated using a HETO vacuum concentrator (Thermo Scientific, A. De Mou, Milano, Italy) for 30 min, to a final volume of 20 μL. A volume of 0.8 μL was spotted onto a Ground Steel MALDI Target Plate (Bruker Daltonik GmbH), allowed to dry, and then followed by an equal volume of 7 mg/mL α-cyano-4-hydroxycinnamic acid.

2.4 Mass spectrometric analysis

For MALDI-MSI analysis, all mass spectra were acquired in linear positive mode in the mass range of 3000–20 000 *m/z* using an UltrafleXtreme (Bruker Daltonik GmbH) MALDI-TOF/TOF MS equipped with a Smartbeam laser operating at 2 kHz frequency. External calibration was performed using a mixture of standard proteins within the mass range of 5500–17 000 *m/z* (ProtMix I, Bruker Daltonics). Images were acquired with a laser diameter of 50 μm and a rastering of 50 μm. For MALDI-MS/MS, representative mass spectra were acquired in reflectron positive mode in the mass range of 700–4500 *m/z*. Precursor ions were selected and fragmented using the laser-induced dissociation and LIFT™ technology and an MS/MS spectra obtained from the accumulation of ∼100 000 laser shots. External calibration was performed using a mixture of standard peptides within the mass range of 750–3500 *m/z* (PepMix I, Bruker Daltonics).

2.5 Histological evaluation

Following MALDI-MSI analysis, the matrix was removed with increasing concentrations of ethanol (70 and 100%) and the slides were stained using trichrome. The slides were then converted to digital format using a ScanScope CS digital scanner (Aperio, Park Center Dr., Vista, CA, USA) and pathological glomerular areas of interest (regions of interest) were highlighted by a pathologist, which included all of the glomeruli and regions manifesting in pathological alterations related to the disease. This allowed for the direct overlap of images and the integration of proteomic and pathological information. The study only compared the profiles glomerular tufts while tubulointerstitial features were not considered for the purpose of the current investigation; specific segmental glomerular areas of fibrosis were included. Globally sclerotic areas were excluded.

2.6 Data analysis

FlexImaging 3.0 (Bruker Daltonics) data, containing spectra of each entire measurement region, were imported into SCiLS Lab 2014 software (http://scils.de/; Bremen, Germany) after the acquisition. SCiLS was used to perform a series of preprocessing steps on the loaded spectra: baseline subtraction (TopHat algorithm) and normalization (total ion current algorithm). A series of further steps was performed in order to generate an average (avg.) spectrum representative of the whole measurement region and of the primary GN subclasses: peak picking (orthogonal matching pursuit algorithm), peak alignment (to align the detected ions with peak maxima), and spatial denoising (http://scils.de/; SCiLS Lab; 8.8 Spatial Denoising). PCA was also performed to reduce the high complexity of the data. Finally, ROC analysis was performed, with an AUC of >0.8 being required, as an

additional criteria to the $p < 0.05$, for a peak to be considered as statistically significant. For MALDI-MS/MS spectra, baseline subtraction and smoothing were performed using FlexAnalysis 3.4 (Bruker Daltonics). All MS/MS spectra were searched against the Swiss-Prot database (Release 2015_05 of Apr 29, 2015) with the Mascot 2.4 search engine (Matrix Science, London, UK). Mass tolerances were set at 2.5–3 Da for MS and 1.4 Da for MS/MS. No enzymes or any fixed post-translational modifications were set in the search parameters.

2.7 Immunohistochemistry with A1AT antibody

In order to confirm the proteomic identification data, a further series of formalin-fixed paraffin-embedded (FFPE) renal biopsies taken from patients with IgAN and FSGS were tested for IHC analysis. This validation group included IgAN with wide sclerosis ($n = 4$), IgAN with a prevalent mesangioproliferative pattern without sclerosis ($n = 4$), and FSGS ($n = 6$). For each specimen, 3 μm thick sections were cut from FFPE blocks. After deparaffinization and rehydration, slides underwent endogenous peroxidase blockage and an antigen retrieval process via EnVision Flex (DAKO). Finally, Autostainer Link 48 (Dako) was used to apply the primary antibody directed against A1AT (polyclonal rabbit, Dako).

3 Results

3.1 Proteomic signatures of primary GN

Initially, the average mass spectra of the entire cohort of patients affected by GN was built within the 3000 to 15 000 m/z mass range. Several of the signals (m/z) present in the spectra had a statistically significant higher intensity ($p < 0.05$ and AUC > 0.8) in primary GN, most specifically signals at m/z 4025, 4048, and 4963, compared with controls (Fig. 1). Moreover, when the specific protein profiles of FSGS, IgAN, and MGN were compared, several signals showed different intensity (Fig. 2A–C). Among them, the intensity of the two signals at m/z 4025 and 4048 was significantly higher in FSGS in comparison to IgAN and MGN (AUC values of 0.84 and 0.82, respectively, Fig. 2A–C). Additionally, the specific protein profile of IgAN showed two signals at m/z 4963 and 5072 with a higher intensity when compared to FSGS, and a higher intensity of signals at m/z 5072 and 6180 when compared to MGN (Fig. 2A–C). Unsupervised PCA was performed on the entire dataset in order to further highlight any proteomic differences between FSGS, MGN, and IgAN, (Fig. 3A). In general, the spectra related to FSGS and IgAN presented distinct distributions, except for one IgAN case (Fig. 3A). The coregistration of the proteomic findings with the histological image highlighted that the group of spectra present in this IgAN patient, which were in common with the spectra from the FSGS cohort, were localized to a distinct group of three sclerotic glomeruli. Therefore, we proceeded with virtual microdissection in order to export spectra from these particular glomeruli and PCA was again performed (Fig. 3B). The spectra exported from these sclerotic glomeruli found within this IgAN patient showed a similar distribution to the entire FSGS cohort in the PCA score chart. In fact, they also showed similar protein profiles, thus strengthening the initial observation that MALDI-MSI has the capability to distinguish individual lesions or subregions of tissue even within an individual form of the studied primary GN. Interestingly, the same IgAN patient identified as more comparable with the FSGS cohort following the PCA presented a similar level of intensity of the two target signals (m/z 4025 and 4048) previously detected as upregulated in FSGS patients (Fig. 2E). Upon viewing the spatial localization of these two signals, they were again correlated with the previously histologically identified sclerotic regions (Fig. 4). Furthermore, these ions also shared

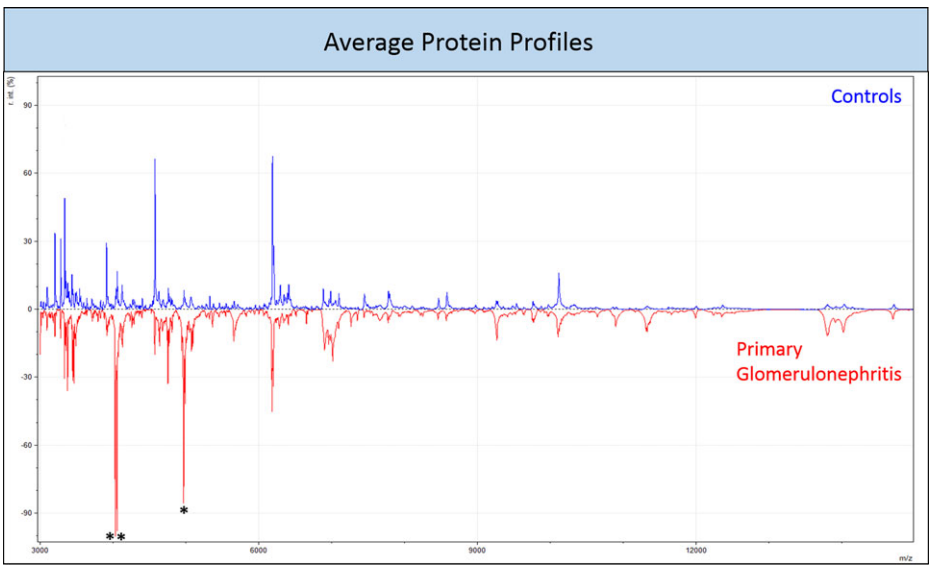

Figure 1. Average protein profiles of healthy renal tissue (top) and from patients with primary glomerulonephritis (bottom) in the 3–15 000 m/z mass range.

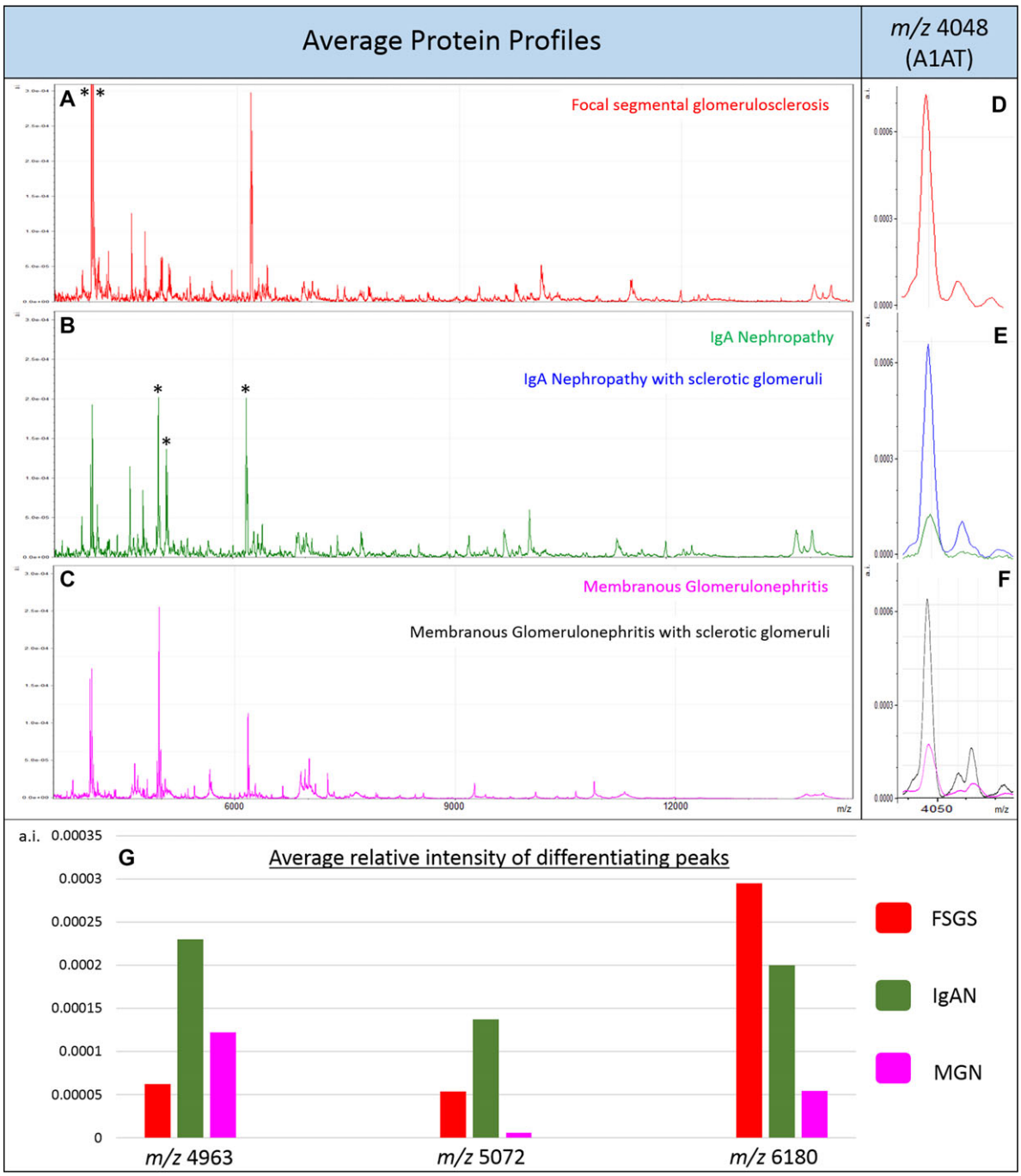

Figure 2. (A–C) Average protein profiles of patients with FSGS (A), IgAN (B), and MGN (C) in the 3–15 000 *m/z* mass range with differentiating peaks (AUC > 0.8) denoted by an asterik. (D–F) Relative intensity of *m/z* 4048 (A1AT) in FSGS (D), IgAN and IgAN with sclerotic glomeruli (E; green and blue, respectively) and MGN and MGN with sclerotic glomeruli (F; fuchsia and black, respectively). (G) The average relative intensity for the three further differentiating peaks (*m/z* 4963, 5072, and 6180) in FSGS, IgAN, and MGN.

a specific sclerosis-related localization within FSGS biopsies (Fig. 4). More interestingly, there was also an individual patient within the MGN group that showed a higher intensity of these signals when compared to the other MGN patients (Fig. 2F). These signals were again well correlated with sclerotic areas within the tissue of this patient.

3.2 Identification of A1AT

The two signals at *m/z* 4025 and 4048 had the capability to discriminate sclerotic glomeruli within different forms of primary GN. Therefore, their identity was investigated by acquiring MS/MS spectra by MALDI-TOF/TOF.

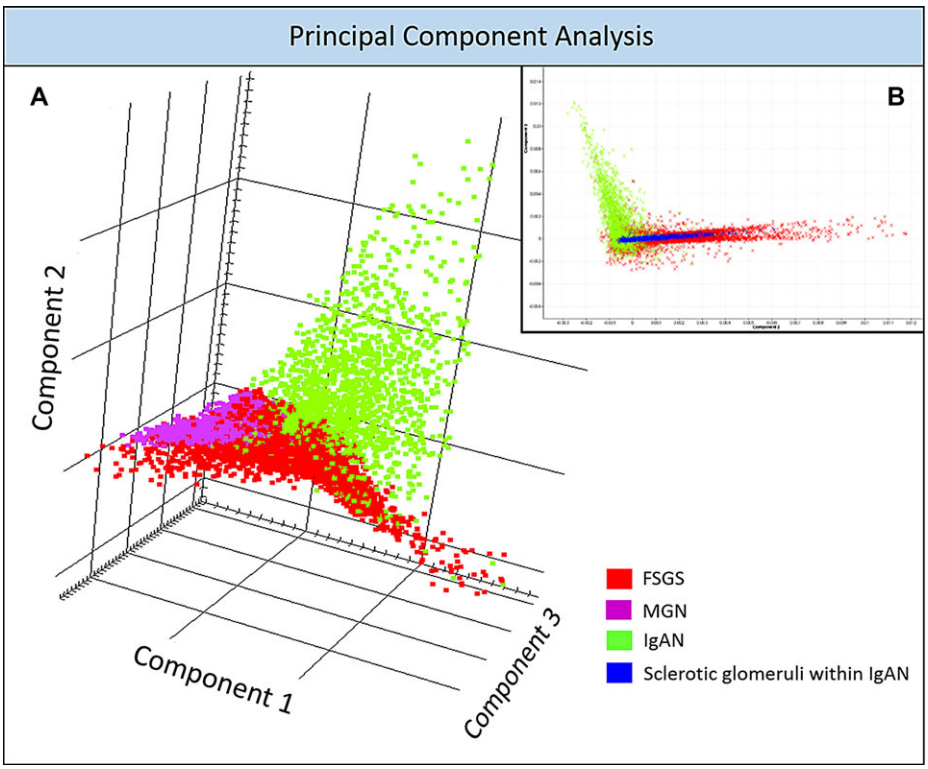

Figure 3. (A) Three-dimensional principal component analysis score chart presenting the distribution of spectra from FSGS (red), MGN (fuchsia), and IgAN (green) patients. (B) Two-dimensional principal component analysis score chart presenting the distribution of spectra from FSGS (red) and IgAN (green) patients along with the distribution of spectra virtually microdissected from sclerotic glomeruli within an IgAN patient (blue).

The peptide fragments in the resulting spectrum were searched against the Swiss-Prot database with the Mascot 2.4 search engine. The signal at *m/z* 4048 was identified as a peptide fragment of A1AT (IPPEVKFNKPFVFLMIEQNTK-SPLFMGKVVNPTQK) with a Mascot score of 77. The IHC staining for A1AT on renal biopsies showed a diffuse positivity among sclerotic areas of FSGS and IgAN and scant positivity/negativity among IgAN with a prevalent mesangioproliferative pattern and controls. Interestingly, in renal biopsies classified as "sclerotic," there was also a strong positivity to A1AT in the cytoplasm of podocytes (Fig. 4). On the contrary, the podocytes present in the renal biopsies with a mesangioproliferative pattern of IgAN and normal glomeruli were completely negative, suggesting that

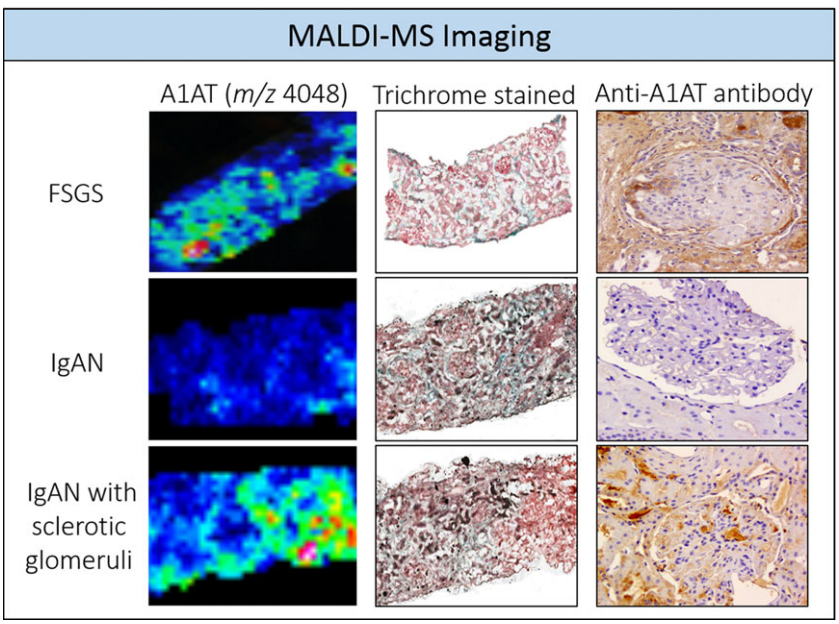

Figure 4. (Left) The molecular distribution of *m/z* 4048 (A1AT) in sections of bioptic renal tissue, obtained using MALDI-MSI, (center) trichrome-stained image of the identical sections used for MALDI-MS imaging and (right) immunohistochemical staining with the anti-A1AT antibody from a validation set of patients. The collection of images is derived from patients with FSGS (top), IgAN (middle), and IgAN with sclerotic glomeruli (bottom).

intraepithelial deposits of A1AT are consistent with a dysfunction of podocytes.

4 Discussion

MALDI-MSI could be the ideal tool for a new approach in investigating GN, both for diagnostic and prognostic purposes. This technique has been reported to be capable of providing specific proteomic profiles for the physiological counterpart and for pathological glomeruli [5]. It can define nosological entities, such as IgAN and FSGS, through their distinctive signatures and could be potentially useful in the biological comprehension of these lesions, supporting the existence of specific molecular alterations. The characterization of the proteomic phenotype of glomeruli is mainly related to the possible clinical development of biomarkers for the prognostic stratification of patients with CKD progression. MALDI-MSI is the newest and most promising imaging method for combining protein/peptide expression with distinct localization inside tissue. In this study, we provide additional evidence of the capability of this technology to discriminate normal kidney from pathological GN, based on specific signals (m/z 4025, 4048, and 4963; Fig. 1) that may represent indicators of CKD development. Moreover, specific disease-related signatures (m/z 4025 and 4048 for FSGS, m/z 4963 and 5072 for IgAN, Fig. 2) were also found. MALDI-MSI showed a common proteomic profile overlap between IgAN and FSGS in sclerotic glomerular regions (Fig. 3). In particular, two specific ions at m/z 4025 and at m/z 4048 were of higher intensity in the sclerotic areas of all FSGS patients as well as in the single IgA patient that presented sclerotic lesions (Fig. 4).

The signal at m/z 4048 was identified by MALDI-TOF/TOF as the resulting peptide fragments belonged to the A1AT protein. A1AT is a major serine proteinase inhibitor (serpin) found in human plasma. It is a glycoprotein with a broad range of activities, including the downregulation of neutrophil elastase during the inflammatory processes. Kwak et al. recently evaluated this protein expression in renal biopsies [6], while other authors independently described its overexcretion in the urine of some patients with primary GNs, most specifically FSGS, IgAN, and minimal change disease [7–9]. The IHC staining against A1AT demonstrated its localization in the cytoplasm of podocytes present in sclerotic glomeruli. This represented an intriguing finding related with possible epithelial dysfunction and consequent insufficient degradation of the extracellular matrix. In this setting, many studies correlated the development of FSGS both with an excessive loss [10] and a hypertrophy of podocytes [11] and A1AT could be one of the markers of podocyte stress, in addition to nephrin, Wilms tumor antigen 1 (WT1), the glomerular epithelial protein 1 (GLEPP1), and thymosin beta-4 [12].

Additionally, the identification of A1AT fragment(s) in urine samples taken from GN patients has been reported [13, 14]. Smaller fragments of the peptide derived from the A1AT protein that we have identified in tissue were also previously detected in urine samples taken from CKD patients. In 2010, Good et al. investigated the urinary peptidome of 230 patients with renal disease and compared them to 379 healthy controls. The authors detected 273 urinary peptides found to be significantly different between cases and controls. Using support vector machines, those potential biomarkers were integrated into a single classifier, called "the CKD 273 classifier," which was validated in several studies for the diagnosis and prognosis of CKD. For three of the detected differentiating ions (m/z 4963, 5072, and 6180), peaks of similar molecular weight were detected in the CKD 273 classifier (personal communication). However, focusing on A1AT, 18 different fragments of this protein were present in the CKD 273 classifier. All of them were upregulated in CKD patients in comparison to the control groups. Five of these fragments partially overlapped with the A1AT fragment we identified in tissue samples. Moreover, urinary A1AT fragments were also found to be correlated with CKD progression in Schanstra et al. The authors of this study performed de novo correlation analysis to investigate which urinary peptides were highly associated with CKD progression (high progression patients were defined on the basis of a decline in percentage of estimated glomerular filtration rate (% eGFR) slope/year $>-5\%$). Thirty-five urinary fragments of A1AT were found to be correlated with baseline eGFR and % eGFR slope/year. Among them, four fragments partially overlapped with the A1AT fragment that we identified in tissue. Moreover, the same A1AT fragment was found to be uprepresented in the urine of another cohort of patients classified as CKD progressors with respect to nonprogressors (data not shown). In this setting, the combined findings from tissue MALDI-MSI and urinary peptidomics provide further agreement with studies that describe the presence of glomerulosclerosis and the aforementioned podocyte changes [10, 11] as early signs of disease progression [15, 16]. Thus, the consistency between tissue and urinary results suggests that A1AT should be further investigated as a putative noninvasive biomarker of CKD progression by studying both bioptic renal tissue and urine from the same patients within a very well-defined cohort that is based upon carefully selected etiologies (FSGN, IgAN, etc.).

In conclusion, this study shows a promising application of MALDI-MSI in the discovery of biomarkers for the assessment of CKD progression. MALDI-MSI not only facilitates the analysis of fresh-frozen specimens but also FFPE tissue, making retrospective studies possible [17]. More specifically, this technology could translate molecular knowledge obtained directly in tissue into routine clinical practice, such as the successful application of the CKD 273 classifier that is based on CE–MS tools.

Furthermore, the localization of A1AT within the sclerotic glomeruli, as highlighted by IHC, reveals that this protein could be related with the so-called "podocyte stress theory" [18–20] and the emerging fibrogenic role of different biomarkers in glomerulosclerosis [11, 12]. Due to some limitations of our study related with the small number of cases analyzed,

further similar studies are needed for a definitive confirmation of this hypothesis and to validate the role of A1AT in GKDs.

This work was supported by grants from the MIUR: FIRB 2007 (RBRN07BMCT_11), FAR 2010–2014; from iMODE-CKD (FP7-PEOPLE-2013-ITN); and in part by the COST Action (BM1104) Mass Spectrometry Imaging: New Tools for Healthcare Research.

The authors have no other relevant affiliation or financial involvements with any organisation or entity with a financial interest in or financial conflict with the subject matter or material discussed in the manuscript apart from those disclosed.

Claudia Pontillo is employed by Mosaiques in the course of a Marie Curie programme and she has no other relevant affiliation or financial involvements with any organisation or entity with a financial interest in or financial conflict with the subject matter or material discussed in the manuscript apart from those disclosed.

5 References

[1] U.S. Renal Data System, USRDS 2013 Annual Data Report: Atlas of Chronic Kidney Disease and End-Stage Renal Disease in the United States. National Institutes of Health, National Institute of Diabetes and Digestive and Kidney Diseases. Bethesda, MD 2013.

[2] Wyatt, R. J., Julian, B. A., IgA nephropathy. *N. Eng. J. Med.* 2013, *368*, 2402–2414.

[3] Orth, S. R., Eberhard, R., The nephrotic syndrome. *N. Eng. J. Med.* 1998, *338*, 1202–1211.

[4] Pagni, F., Galimberti, S., Goffredo, P., Basciu, M. et al., The value of repeat biopsy in the management of lupus nephritis: an international multicentre study in a large cohort of patients. *Nephrol. Dial. Transplant.* 2013, *28*, 3014–3023.

[5] Mainini, V., Pagni, F., Ferrario, F., Pieruzzi, F. et al., MALDI imaging mass spectrometry in glomerulonephritis: feasibility study. *Histopathology* 2014, *64*, 901–906.

[6] Kwak, N. J., Wang, E. H., Heo, I. Y., Jin, D. C. et al., Proteomic analysis of alpha-1-antitrypsin in immunoglobulin A nephropathy. *Proteomics Clin. Appl.* 2007, *1*, 420–428.

[7] Navarro-Muñoz, M., Ibernón, M., Bonet, J., Pérez, V. et al., Uromodulin and α(1)-antitrypsin urinary peptide analysis to differentiate glomerular kidney diseases. *Kidney Blood Press. Res.* 2012, *35*, 314–325.

[8] Graterol, F., Navarro-Muñoz, M., Ibernón, M., López, D. et al., Poor histological lesions in IgA nephropathy may be reflected in blood and urine peptide profiling. *BMC Nephrol.* 2013, 14:82. doi: 10.1186/1471-2369-14-82.

[9] Pérez, V., Ibernón, M., López, D., Pastor, M. C. et al., Urinary peptide profiling to differentiate between minimal change disease and focal segmental glomeurlosclerosis. *PLoS One* 2014, *9*, e87731. doi: 10.1371/journal.pone.0087731.

[10] Lemley, K. V., Lafayette, R. A., Safai, M., Derby, G. et al., Podocytopenia and disease severity in IgA nephropathy. *Kidney Int.* 2002, *61*, 1475–1485.

[11] Wiggins, J. E., Goyal, M., Sanden, S. K., Wharram, B. L. et al., Podocyte hypertrophy, "adaptation," and "decompensation" associated with glomerular enlargement and glomerulosclerosis in the aging rat: prevention by calorie restriction. *J. Am. Soc. Nephrol.* 2005, *16*, 2953–2966.

[12] Xu, B. J., Shyr, Y., Liang, X., Ma, L. J. et al., Proteomic patterns and prediction of glomerulosclerosis and its mechanisms. *J. Am. Soc. Nephrol.* 2005, *16*, 2967–2975.

[13] Good, D. M., Zurbig, P., Argiles, A., Bauer, H. W. et al., Naturally occurring human urinary peptides for use in diagnosis of chronic kidney disease. *Mol. Cell. Proteomics* 2010, *9*, 2424–2437.

[14] Schanstra, J. P., Zurbig, P., Alkhalaf, A., Argiles, A. et al., Diagnosis and prediction of CKD progression by assessment of urinary peptides. *J. Am. Soc. Nephrol.* 2015, *26*, 1999–2010.

[15] Barton, M., Tharaux, P. L., Endothelin and the podocyte. *Clin. Kidney J.* 2012, *5*, 17–27.

[16] Kriz, W., Lemley, K. V., A potential role for mechanism forces in the detachment of podocytes and the progression of CKD. *J. Am. Soc. Nephrol.* 2015, *26*, 258–269.

[17] De Sio, G., Smith, A. J., Galli, M., Garancini, M. et al., A MALDI-mass spectrometry imaging method applicable to different formalin-fixed paraffin-embedded human tissues. *Mol. Biosyst.* 2015, *11*, 1507–1514.

[18] Smeets, B., Moeller, M. J., Parietal epithelial cells and podocytes in glomerular diseases. *Semin. Nephrol.* 2012, *32*, 357–367.

[19] Moeller, M. J., Smeets, B., Role of parietal epithelial cells in kidney injury: the case of rapidly progressing glomerulonephritis and focal and segmental glomerulosclerosis. *Nephron Exp. Nephrol.* 2014, *126*, 97–100.

[20] Kretzler, M. Role of podocytes in focal sclerosis: defining the point of no return. *J. Am. Soc. Nephrol.* 2005, *16*, 2830–2832.

7.4 My curriculum vitae does not appear in the electronic version of my paper for reasons of data protection

7.5 Complete list of publications

1. **Filip S**, Pontillo C, Peter Schanstra J, Vlahou A, Mischak H, Klein J. Urinary proteomics and molecular determinants of chronic kidney disease: possible link to proteases. Expert review of proteomics. 2014;11(5):535-48.
2. **Filip S**, Zoidakis J, Vlahou A, Mischak H. Advances in urinary proteome analysis and applications in systems biology. Bioanalysis. 2014;6(19):2549-69.
3. Pontillo C, **Filip S**, Borras DM, Mullen W, Vlahou A, Mischak H. CE-MS-based proteomics in biomarker discovery and clinical application. Proteomics Clinical applications. 2015;9(3-4):322-34.
4. Glorieux G, Mullen W, Duranton F, **Filip S**, Gayrard N, Husi H, Schepers E, Neirynck N, Schanstra JP, Jankowski J, Mischak H, Argiles A, Vanholder R, Vlahou A, Klein J. New insights in molecular mechanisms involved in chronic kidney disease using high-resolution plasma proteome analysis. Nephrology, dialysis, transplantation: official publication of the European Dialysis and Transplant Association - European Renal Association. 2015;30(11):1842-52.
5. **Filip S**, Vougas K, Zoidakis J, Latosinska A, Mullen W, Spasovski G, Mischak H, Vlahou A, Jankowski J. Comparison of Depletion Strategies for the Enrichment of Low-Abundance Proteins in Urine. PloS one. 2015;10(7):e0133773.
6. Smith A, L'Imperio V, De Sio G, Ferrario F, Scalia C, Dell'Antonio G, Pieruzzi F, Pontillo C, **Filip S**, Markoska K, Granata A, Spasovski G, Jankowski J, Capasso G, Pagni F, Magni F. alpha-1-antitrypsin detected by MALDI-Imaging in the study of glomerulonephritis: its relevance in chronic kidney disease progression. Proteomics. 2016.

7.6. Acknowledgements

At this point, I would like to thank all who have contributed to this work. I would like to express my special thanks and appreciation to:

- Prof. Dr. Joachim Jankowski for all the support and assistance as well as for the corrections of the thesis
- Dr. Antonia Vlahou for the continuous guidance, advice, help and motivation during the project
- Dr. Jerome Zoidakis for all the motivation, advice and support
- Prof. Dr. Harald Mischak for all the support, guidance and advice
- Dr. William Mullen for teaching me how to use mass-spectrometry instruments and for performing the LC-MS/MS runs
- Dr. Konstantinos Vougas for the encouraging discussions regarding data analysis as well as performing the LC-MS/MS runs
- Dr. Giorgos Mermelekas for the time spent explaining to me targeted proteomics approaches, his support in analysing the samples as well as for performing the MRM runs
- Dr. Julie Klein for the teaching me how to analyse large-scale datasets
- Dr. Manousos Makridakis for all the help with resolving any problems that occurred during the wet-lab sample preparation procedures
- Ms. Vasiliki Lygirou for all the help with performing the wet-lab experiments
- Ms. Magdalena Krochmal for the encouraging discussions related to the application of programming languages
- Ms. Agnieszka Latosinska for the support and time spent explaining how to analyse proteomics data
- All the members of the proteomics laboratory in Biomedical Research foundation of the Academy of Athens for their help in any aspects of the project as well as for their friendly collaboration
- All the partners of the iMODE-CKD consortium for many interesting discussions and interesting collaborations